Hybrid Inverse Problems Arising from Acousto-Electric Coupling

Ilker Kocyigit

A dissertation submitted in partial fulfillment of the requirements for the degree of

Doctor of Philosophy

University of Washington

2013

Reading Committee:

Gunther Uhlmann, Chair

Kenneth P. Bube

Hart Smith

Program Authorized to Offer Degree:
Mathematics

University of Washington

Abstract

Hybrid Inverse Problems
Arising from Acousto-Electric Coupling

Ilker Kocyigit

Chair of the Supervisory Committee:
Professor Gunther Uhlmann
Mathematics

We study hybrid imaging techniques that aim to overcome the ill-posedness of the Electric Impedance Tomography using the acousto-electric coupling. For the isotropic case, we consider the problem of reconstructing the internal conductivity of an object by making electric measurements on the boundary while perturbing the conductivity by sending ultrasound waves to the object. The conductivity can be uniquely recovered by using one boundary potential. To obtain the uniqueness, the problem is reduced to an inverse problem with internal data. Lipschitz type stability results for certain internal data are also discussed. In the last part of this thesis we discuss similar inverse problems in more general settings.

TABLE OF CONTENTS

Page

LIST OF FIGURES

LIST OF TABLES

ACKNOWLEDGMENTS

I would like to express my gratitude to my advisor, Gunther Uhlmann, for all his support and encouragement during my graduate study. I would like to thank the members of my committee. Last, but not least, my special thanks go to my family members for the support and understanding they provided me.

DEDICATION

to my dear wife, Betul

Chapter 1

INTRODUCTION AND BACKGROUND

1.1 Introduction and Organization

The behavior of a conductive object when an electromagnetic field is present can be described by its electrical properties such as the electrical conductivity, permittivity and permeability. These can be used to extract useful information about the object. Imaging the inhomogeneities of these electrical properties have many uses, for example, in detection of a unhealthy tissue in medical imaging. The conductivity of a cancerous tissue can be 6 times higher than the healthy tissue (the permittivity can be 3.8 times higher [24],[39]), and therefore the conductivity map can be very helpful when it is used for the detection of unhealthy tissues. Another example is in geophysical imaging, in fact, motivated by geophysical prospection Calderón gave mathematical formulation of the inverse problem of recovering the conductivity map from the knowledge of the electric measurements on the boundary of the object [16]. This problem is known as *Calderón's problem* (or inverse conductivity problem) and the inverse method is known as *electrical impedance tomography* (EIT). EIT is a low cost, non penetrating and safe modality and it has many potential application areas. In addition to medical imaging and geophysics it is also used in environmental sciences and nondestructive testing of materials. Since Calderón's paper there has been extensive study on EIT, see [68], [14], [19] for reviews of the theoretical and numerical studies of the inverse problem of EIT.

A major breakthrough in Calderón's problem was in [65], [66] where Sylvester and Uhlmann used a set of special exponentially growing solutions, called complex geometrical optics solutions, to show that the conductivity can be uniquely reconstructed from the boundary measurements when dimension is $n \geqslant 3$ and conductivity map is C^2. Although

the conductivity can uniquely be recovered, unfortunately EIT is a severely ill-posed inverse problem [1], and implementations of EIT yield poor resolution images of conductivity. Therefore it makes it less usable for applications such as medical imaging which typically requires resolution in the sub-millimeter levels. In order to overcome the ill-posedness and the resolution limitations of such problems a new type of inverse problems called Hybrid Inverse Problems have been studied recently. They are also referred as coupled physics, interior data or multi-wave problems. Hybrid imaging techniques usually aim to combine the advantages of two different modalities and eliminate their limitations. The key point in combining the advantage of each modality is making use of the physical coupling between them instead of applying each separately. Acousto-Electric Tomography (AET, also called ultrasound modulated electrical impedance tomography or UM-EIT), Photo-acoustic Tomography (PAT) and Thermo-Acoustic Tomography (TAT) are some of the examples of hybrid methods that aims to produce high contrast high resolution images of the unknown coefficients by making use of two different modalities. Other examples include Ultrasound Modulated Optical Tomography (UMOT, also known as Acousto-Optic Tomography or AOT), Magnetic Resonance EIT (MREIT) or Current Density Impedance Imaging (CDII), and Transient Elastography (TE).

Hybrid inverse problems usually consist of two steps. Typically in the first step an internal data is obtained by one of the modalities which is usually the high-resolution and low-contrast one of the two. For example in AET this step involves the ultrasound, and in PAT and TAT it involves solving an inverse problem for wave equation. We will give references on AET in the following sections, and more information about various Hybrid Inverse Problems can be found in the following articles and books [63], [10], [46], [71], [60], [21]. As in typical inverse problems, the main questions addressed by these hybrid inverse problems are;

– Uniqueness : Can two distinct properties (inhomogeneity maps such as conductivity) produce the same boundary measurement results ?

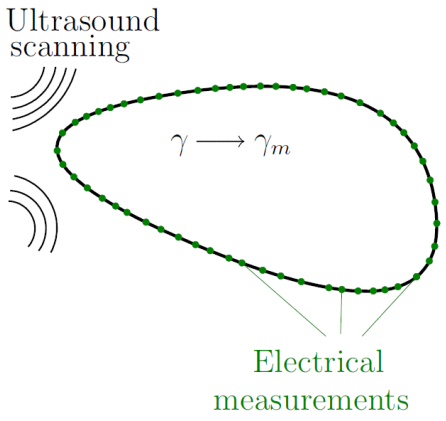

Figure 1.1: Ultrasound scanning causes a small change in conductivity due to electro-acoustic effect and this causes a change in the current readings on the boundary. γ is the conductivity map and γ_m is the 'modulated' conductivity.

- Stability : Does the closeness of two measurement data imply the closeness of the inhomogeneity maps ?

- Construction or reconstruction : Is there an algorithm to construct the inhomogeneity map from the known measurement data ?

As a hybrid inverse problem, AET aims to inherit the high contrast from electrical modality and high resolution from ultrasound, and it is introduced to overcome the ill-posedness of EIT by making use of the coupling between electromagnetic waves and acoustic waves. It is known that when ultrasound waves are sent to a conductive object, they cause a small change in the conductivity [72]. This phenomenon is called acousto-electric coupling, and it can be detected by making boundary measurements, for example in an EIT experiment such a change in the conductivity will change the steady current of the experiment and thus perturb the current readings on the boundary. The main subject of this thesis is AET and related hybrid inverse problems that are arising from acousto-electric coupling. The organization of this thesis is as follows.

– Chapter 1. We give necessary introduction on EIT problem and the Acousto-Electric modulation.

– Chapter 2. We describe and discuss the AET problem and some of the previously known results. The main purpose of this chapter is to study the AET problem in the following setting :

  i. the conductivity is scalar,

  ii. the measurements are coming from one fixed boundary potential f.

  The rest of Chapter 2 follows [43], where the author propose two separate methods to recover two different internal data from the boundary measurements. The first one is an internal data of the form $\gamma^{1/2}\nabla u$, and the second is $\gamma\nabla u$ (i.e. the current). The first internal data is recovered using CGO solutions and useful for theoretical considerations such as uniqueness, the latter is recovered assuming that $\nabla\gamma/\gamma$ is small under suitable norms. Next stability estimates for the recovery of the conductivity are discussed and Lipschitz type stability estimates are presented. One is achieved by reducing the problem to the transport equation and using ODE based techniques, and another by a PDE based approach. Although the internal data are in different forms, the corresponding second steps (i.e. inverse problem with internal data) are similar. Finally, several numerical examples are presented to study inversion algorithms (based on the constructive proofs of the results) of both steps and the effectiveness of the algorithms under noisy data sets.

– Chapter 3. We discuss some possible generalizations of the problem. One of these generalizations is to consider steady state case but with anisotropic conductivity. We give approximation algorithm when the conductivity is close to identity, i.e. local reconstruction. We also discuss the case of the partial data when the ultrasound scanning might be assumed to be restricted to some part of the domain. Another general

setting for the same problem can be derived by using time-harmonic electromagnetic waves instead of the steady state case. In this setting, we use Maxwell's equations with the assumption that the permittivity, conductivity, and permeability are scalar functions. We also assume that one is able to make deformations on these coefficients locally and try to recover them by making electromagnetic measurements on the boundary.

In the rest of this section we give brief information on the notation used in the following sections of this work. $\hat{f}$ denotes the Fourier Transform of a distribution f. Similar notation used for the normalized vector, i.e. $\hat{\rho} := \frac{\rho}{|\rho|}$ for any $\rho \in \mathbb{R}^n$. $H^s(\Omega)$ denotes the Sobolev space (see [67] or [23]) and sometimes H^s is used instead of $H^s(\mathbb{R}^n)$. Similarly for other spaces, when domain is not specified it is understood $\mathbb{R}^n$. When $s \geqslant 0$ is an integer H^s is defined by

$$H^s(\mathbb{R}^n) = \{u \in S'(\mathbb{R}^n) : \langle \xi \rangle^s \hat{u} \in L^2(\mathbb{R}^n)\}$$

where S' is the space of tempered distributions and

$$\langle x \rangle = (1 + |x|^2)^{1/2}$$

for $x \in \mathbb{R}^n$. When $s > 0$ H^s can be defined by interpolation of Banach spaces. Suppose Ω is a subset of $\mathbb{R}^n$ with smooth boundary. Then, $H_0^s(\Omega)$ is defined as the completion of $\{u \in C_c^\infty(\Omega)\}$ under the H^s norm for $s \geqslant 0$. Here $C_c^\infty(\Omega)$ denotes the smooth functions which are compactly supported in domain Ω. For $s \geqslant 0$, $H^s(\Omega)$ is the completion of $\{u \in C^s(\Omega) : \|u\|_{H^s(\Omega)} < \infty\}$ under the norm

$$\|u\|_{H^s(\Omega)} = \left\{ \sum_{\alpha \leqslant s} \int_\Omega |D^\alpha u(x)|^2 \mathrm{d}x \right\}^{1/2}.$$

As above, for real $s > 0$, $H^s(\Omega)$ can be defined by interpolation of Banach spaces. When s is a negative integer we define $H^s(\Omega)$ to be the dual space $(H_0^{-s}(\Omega))^*$, that is the space of bounded linear functionals on $H_0^{-s}(\Omega)$. $H^s(\Omega)$ is then a Hilbert space equipped with the

inner product which is induced from its norm. $H^s(\partial\Omega)$ is defined by covering the boundary $\partial\Omega$ with local coordinate patches and using the above definitions on the local coordinates.

The space L^2_δ is called *the weighted L^2 space* and defined as the completion of $C^\infty_c(\mathbb{R}^n)$ with respect to the norm $\|\cdot\|_{L^2_\delta}$ which is given by

$$\|h\|_{L^2_\delta} = \left(\int_{\mathbb{R}^n} \langle x\rangle^{2\delta}|h(x)|^2 \mathrm{d}x\right)^{1/2}.$$

This is a summability condition about ∞, therefore if Ω is a bounded domain then for all $h \in L^2_\delta$ supported in Ω

$$C_\Omega^{-1}\|h\|_{L^2} \leqslant \|h\|_{L^2_\delta} \leqslant C_\Omega\|h\|_{L^2},$$

where C_Ω is independent of h, that is the norm L^2_δ is equivalent to L^2. Define H^s_δ for $s \geqslant 0$ as the completion of $C^\infty_c(\mathbb{R}^n)$ with respect to the norm $\|\cdot\|_{H^s_\delta}$ which is defined as

$$\|u\|_{H^s_\delta} = \|\langle x\rangle^\delta (I-\Delta)^{s/2}u\|_{L^2}.$$

Note that when $\delta = 0$, H^s_δ is equivalent to the Sobolev norm H^s.

1.2 EIT and Complex Geometrical Optics Solutions

In this section we discuss the complex geometrical optics (CGO) solutions together with the EIT which is the first inverse problem where CGO solutions are applied.

1.2.1 Forward and Inverse Conductivity Problem

Let Ω be a bounded domain with smooth boundary $\partial\Omega$ and γ be a real valued measurable function with

$$\frac{1}{C_0} < \gamma(x) < C_0, \tag{1.1}$$

defined on Ω. Define the differential operator

$$L_\gamma(u) = \nabla\cdot(\gamma\nabla u).$$

Given a function $f \in H^{1/2}(\partial\Omega)$, consider the weak solution $u \in H^1(\Omega)$ of the following boundary value problem

$$\begin{cases} L_\gamma(u) = 0, \text{in}\,\Omega \\ u|_{\partial\Omega} = f. \end{cases} \tag{1.2}$$

When γ is known the problem of finding u from a given boundary value f is called *the (forward) conductivity problem* in regards to the electrical prospection problem it is originating from. In more general settings γ is considered as a symmetric, positive definite matrix valued function and in that case it is called *anisotropic conductivity*. In this section we consider the isotropic case, i.e. γ is a scalar function. We give more details about the anisotropic case in the last chapter when we study an anisotropic extension of inverse problem of AET. The map

$$\Lambda_\gamma : f \to \gamma\nabla u|_{\partial\Omega}$$

is called Dirichlet-to-Neumann map (or voltage-to-current map) where u is the solution of (1.2) for a given boundary value f. When γ is a smooth function $\Lambda_\gamma(f) = \gamma\nabla u|_{\partial\Omega}$ is well defined and if $f \in H^{1/2}(\partial\Omega)$ then by bounded linear transformation theorem Λ_γ extends to a linear map from $H^{1/2}(\partial\Omega)$ to $H^{-1/2}(\partial\Omega)$. An application of divergence theorem shows that one can weakly define the functional $\Lambda_\gamma f$ as

$$\langle \Lambda_\gamma f, g\rangle := \int_\Omega \gamma\nabla u_f \cdot \nabla u_g \mathrm{d}x$$

where $f \in H^{1/2}(\partial\Omega)$, $g \in H^{1/2}(\partial\Omega)$ and u_g is an extension of g, and u_f is the solution of (1.2). The Calderón's problem is then to recover γ from the knowledge of Λ_γ. Note that knowing Λ_γ corresponds to knowing the current response of the object for every possible boundary potential f. As introduced in the previous section, EIT aims to image the conductivity map of an object and it is mathematically modeled by the inverse conductivity problem.

In [16], Calderón defined the quadratic form

$$Q_\gamma(f) := \int_\Omega \gamma(x)|\nabla u(x)|^2 \mathrm{d}x$$

where u is the solution of (1.2) and he raised the question whether $\Phi : \gamma \to Q_\gamma$ is an injective map. This is restatement of the inverse conductivity problem since the knowledge of Λ_γ is equivalent to the knowledge of Q_γ by polarization. He didn't show the injectivity of Φ, instead he linearized the problem and showed that the operator $\delta \to \mathrm{d}\Phi|_{\gamma=\text{constant}}$ is injective. It can be seen that when γ is constant, the Fréchet derivative of Φ at δ is the linear operator

$$\mathrm{d}\Phi|_{\gamma=1}(\delta): \quad f \mapsto \int_\Omega \delta(x)|\nabla u(x)|^2 \mathrm{d}x$$

where u is the harmonic function on Ω with $u|_{\partial\Omega} = f$. In order to show this linearized operator is injective one needs to prove that if $\mathrm{d}\Phi|_{\gamma=1}$ vanishes for all f then δ also vanishes. This is equivalent to showing

$$\int_\Omega \delta(x)\nabla u_1(x)\cdot\nabla u_2(x)\mathrm{d}x = 0, \forall u_1, u_2 \in H \qquad \Longrightarrow \qquad \delta = 0 \tag{1.3}$$

where H denotes the harmonic functions on Ω. The idea of Calderón was using special harmonic functions of the form

$$u_1(x) = e^{(\xi+ik)\cdot x}, \quad u_2(x) = e^{(-\xi+ik)\cdot x}, \tag{1.4}$$

where $\xi, \eta \in \mathbb{R}^n$ such that $|\xi| = |\eta|$ and $\xi \cdot \eta = 0$. Substituting these functions in (1.3) gives $c|k|^2(\chi_\Omega\delta)\widehat{\ }(k) = 0$ for any $k \in \mathbb{R}^n$ where χ_Ω is the characteristic function of domain Ω. Thus $\delta = 0$ which shows the injectivity of $\mathrm{d}\Phi$.

Complex Geometrical Optics

Since the solutions Calderón used are harmonic, the above method is valid only if γ is constant. Sylvester and Uhlmann [65], [66] showed that this idea can be extended to general conductivities by using more general functions which are not harmonic but the perturbations of the solutions of the form (1.4). Using these functions they showed that, not only the linearized operator but also the original operator $\Phi : \gamma \to Q_\gamma$ is injective, which gives affirmative answer to the question raised by Calderón. A change of variables shows that the

conductivity equation $L_\gamma v = 0$ is equivalent to the Schrödinger equation

$$\Delta u_\rho - q u_\rho = 0 \tag{1.5}$$

where

$$q = \frac{\Delta\sqrt{\gamma}}{\sqrt{\gamma}} \text{ and } u = \sqrt{\gamma} v$$

assuming $\gamma \in C^2(\Omega)$. Moreover 0 is not a Dirichlet eigenvalue of $(\Delta - q)$, thus above system has a unique solution for any Dirichlet data in $H^{1/2}(\partial\Omega)$. We denote q as the conductivity for Schrodinger equation.

CGO solutions are special solutions to (1.5) which behave like $e^{\rho\cdot x}$ as $|\rho|$ tends to ∞. They are important tools that are proven to be useful for various inverse problems. They are the solutions to (1.5) of the form

$$u(x) = e^{\rho\cdot x}(1 + \psi_\rho(x))$$

which have the essential properties of $e^{\rho\cdot x}$ as $|\rho| \to \infty$ so that they can be used similarly as in Calderón's argument [66]. For more details we refer the reader to [65], [66] and [53] where CGO solutions are used to solve the inverse conductivity problem. The following is an existence theorem for CGO solutions.

Theorem 1. *Let $-1 < \delta < 0$. There exists $\varepsilon = \varepsilon(\delta)$ and $C = C(\delta)$ such that, for every $q \in L^2_{\delta+1}$ with $\langle x\rangle q \in L^\infty$ and $\rho \in \mathbb{C}^n$ with $\rho\cdot\rho = 0$ satisfying*

$$\|\langle x\rangle q\|_{L^\infty} + 1 \leqslant \varepsilon|\rho|$$

there exists a unique solution to

$$\Delta u + qu = 0 \text{ in } \mathbb{R}^n$$

of the form

$$u(x) = e^{\rho\cdot x}(1 + \psi_\rho(x))$$

where $\psi_\rho(x) \in L^2_\delta$. Furthermore,

$$\|\psi_\rho\|_{L^2_\delta} \leqslant \frac{C}{|\rho|}\|q\|_{L^2_{\delta+1}}.$$

The following proposition from [11] is useful for the existence of more regular CGO solutions.

Proposition 2. *([11], Proposition 3.1 and its corollary) Let $\rho \in \mathbb{C}^n$ such that $\rho \cdot \rho = 0$. Set $s = \frac{n}{2} + \Bbbk + \varepsilon$. Let $-1 < \delta < 0$ and $k \in \mathbb{N}^*$. Let $q \in H^s_1$ and hence in $H^s_{\delta+1}$ and ρ satisfy*

$$\|q\|_{H^s_1} + 1 \leqslant \eta|\rho|. \tag{1.6}$$

Then $u_\rho(x) = e^{\rho\cdot x}(1 + \psi_\rho(x))$ is the unique solution to (1.5) and $\psi_\rho \in H^s$ satisfy

$$\|\psi_\rho\|_{H^s_\delta} \leqslant \frac{C}{|\rho|}\|q\|_{H^s_{\delta+1}},$$

for a constant C that depends on δ and η.

Moreover, on domain Ω, we have

$$|\rho|\|\psi_\rho\|_{H^s(\Omega)} + \|\psi_\rho\|_{H^{s+1}(\Omega)} \leqslant C\|q\|_{H^s(\Omega)}. \tag{1.7}$$

Remarks.

i. On a bounded domain the result of the above theorem can be restated as

$$\|\psi_\rho\|_{L^2(\Omega)} \leqslant \frac{C}{|\rho|}\|q\|_{L^2(\Omega)} \text{ and } \|\psi_\rho\|_{H^1(\Omega)} \leqslant C\|q\|_{L^2(\Omega)}$$

for every $q \in L^\infty(\Omega)$, and $u \in H^2(\Omega)$. This can be seen by an application of interior elliptic regularity. Recall that interior elliptic regularity gives higher order regularity estimates for the solution such as

$$\|u\|_{H^l(\Omega)} \leqslant C(\|F\|_{H^{l-2}(\Omega')} + \|u\|_{L^2(\Omega')})$$

where $\bar{\Omega} \subset \Omega$ are both bounded subsets of $\mathbb{R}^n$ with smooth boundaries, u is the solution to $(\Delta - q)u = F$ in our case. Here C is depending on Ω, Ω', l and q.

ii. The Sobolev embedding and (1.7) together give

$$|\rho|\|\psi_\rho\|_{C^\Bbbk(\bar{\Omega})} + \|\psi_\rho\|_{C^{\Bbbk+1}(\bar{\Omega})} \leqslant C\|q\|_{H^s(\Omega)}. \tag{1.8}$$

Suppose we are given $\sqrt{\gamma} \in H^{s+2}(\Omega)$. Then there exists a bounded extension operator from $H^{s+2}(\Omega)$ to $H^{s+2}(\mathbb{R}^n)$ (see for example [23]). We thus can assume $\sqrt{\gamma} \in H^{s+2}(\mathbb{R}^n)$. This implies that $q \in H^s$ in since H^s is an algebra and $\frac{1}{\sqrt{\gamma}} \in H^{s+2}$. Note that on the bounded domain Ω, $\langle x \rangle$ is bounded from above and below by positive constants so that $q \in H_1^s(\Omega)$. We say v=$\gamma^{-1/2} e^{\rho \cdot x}(1 + \psi_\rho(x))$ is the *CGO solution for* ρ of the conductivity equation if ρ, q and ψ_ρ satisfy the conditions given in Proposition 2.

Given two conductivities γ_1, γ_2 on Ω, the equality of Dirichlet-to-Neumann maps implies that

$$D^\alpha \gamma_1 = D^\alpha \gamma_2$$

on the boundary $\partial\Omega$ for any multi-index α ([45]). This implies that for any two solutions u_1, u_2 of (1.5) one has

$$\int_\Omega (q_1 - q_2) u_1 u_2 \mathrm{d}x = 0 \tag{1.9}$$

where

$$q_1 = \frac{\Delta\sqrt{\gamma_1}}{\sqrt{\gamma_1}}, q_2 = \frac{\Delta\sqrt{\gamma_2}}{\sqrt{\gamma_2}}$$

are coefficients for the above Schrödinger equation. Then showing the injectivity of the nonlinear operator reduces to showing that (1.9) implies $q_1 = q_2$. This is because $q_1 = q_2$ implies $\gamma_1 = \gamma_2$ in the account of the fact that (1.5) admits unique solution for a given boundary value. Note that the statement that (1.9) implies $q_1 = q_2$ is in fact a density argument which is true if the multiplications of solutions u_1, u_2 are dense in $L^2(\Omega)$. This is shown by means of CGO solutions; Let ρ_1, ρ_2 satisfy the conditions of Theorem 1 and let u_1, u_2 be the corresponding solutions for ρ_1, ρ_2 respectively as in Theorem 1. Moreover assume that $\rho_1 + \rho_2 = ik$ for some given $k \in \mathbb{R}^n$, then the decay condition given in Theorem 1 implies that

$$u_1 u_2 = e^{ik \cdot x} + O\left(\frac{1}{|\rho|}\right)$$

in $L^2(\Omega)$. Then, letting $|\rho| \to \infty$ and using arguments similar to Calderón's as above gives $(q_1 - q_2) = 0$ on Ω. Note that the above conclusion assumes that for any given k there

exist ρ_1, ρ_2 satisfying conditions of Theorem 1 such that $\rho_1 + \rho_2 = ik$, in fact such a freedom exists only if $n \geqslant 3$. The following is the main injectivity given in [66] for C^2 conductivities.

Theorem 3. *Suppose* $\gamma_1, \gamma_2 \in C^2(\bar{\Omega})$ *such that* $0 < C^{-1} < \gamma_i < C$ *and* $n \geqslant 3$. *Then* $\gamma_1 = \gamma_2$ *implies* $\Lambda_{\gamma_1} = \Lambda_{\gamma_2}$.

The above theorem gives a uniqueness result, unfortunately EIT is an ill-posed inverse problem in the sense that it has logarithmic type stability. In [1] it is proven that when $n \geqslant 3$ and

$$\|\gamma\|_{H^s(\Omega)} \leqslant C \text{ with } s > \frac{n}{2} + 2$$

then γ depends on the operator Λ_γ continuously but the modulus of continuity is logarithmic. In fact this logarithmic type stability estimate is the best estimate one can expect in general which is proved in [50] by constructing examples when $\|\gamma\|_{C^k(\bar{\Omega})} \leqslant C$ for any finite $k \in \mathbb{N}$ and $n \geqslant 2$.

In the inverse problems one usually have limited information about the solutions of the corresponding 'forward' boundary value problem since the coefficients are not known. However some set of boundary values can imply that the corresponding solutions may have certain qualitative properties which can be very useful. CGO solutions can also be used to construct such useful sets. An example is from [11]. The authors require a field β to satisfy a certain property (more precisely integral curves of β maps a point inside the domain to a point on the boundary in finite time). Moreover this field β depends on two unknown solutions of the boundary value problem. For arbitrary solutions this property may not be satisfied for β. In order to control β, the authors use the CGO solutions and their property that they have sufficiently "flat" gradients when $|\rho|$ is large. Another similar example, given in the problem of TAT, is using the trace of a CGO solution as a boundary data to make a map a contraction.

1.3 Acousto-electric modulation

In this section we introduce the acousto-electric coupling and how it can be used to overcome the ill-posedness of inverse conductivity problem. We assume γ isotropic and the more general cases is discussed in the last chapter. The ultrasound waves can penetrate deep into tissues and can provide high resolution but with a lower contrast. Therefore a method that can combine resolution strength of ultrasound and contrast of electrical properties seems promising. AET is proposed for this aim in [72].

In AET a fixed potential is applied to the boundary of the object under inspection, then ultrasound waves are sent which cause a small change in the conductivity of the object due to the acousto-electric effect. The induced current on the boundary is measured before and after this perturbation. The difference between these two values is observable and measured as data in the AET setting and the inverse problem is to recover the conductivity map from the knowledge of this data. The resulting inverse problem is much more stable compared to EIT. As mentioned in [48], the location of the perturbation of conductivity, which is an extra information that we don't have in the case of EIT, has a stabilizing effect on the inverse problem. Inverse problems arising from AET have been studied recently in [3], [4], [48], [47], [5], [17], [5], [9], [72], [25], [43], [8]. In Figure 1.2, the first image shows the modulation function m where the change in conductivity is modeled by $\gamma_m = (1+m)\gamma$, the second image shows the change in the current caused by the modulation when boundary potential is fixed, the last image shows the change in current readings on a part of the boundary. The goal is to construct the conductivity from this boundary data. The conductivity profile used to generate these images is presented in Figure 2.2 in following sections.

In AET the first step is usually extraction of an internal information; A fixed potential f is applied to the boundary, then, by making electro-acoustic measurements mentioned above, a functional (defined on the domain) is constructed. Although it is constructed without penetrating into the object, this functional is referred as *internal data* since it contains

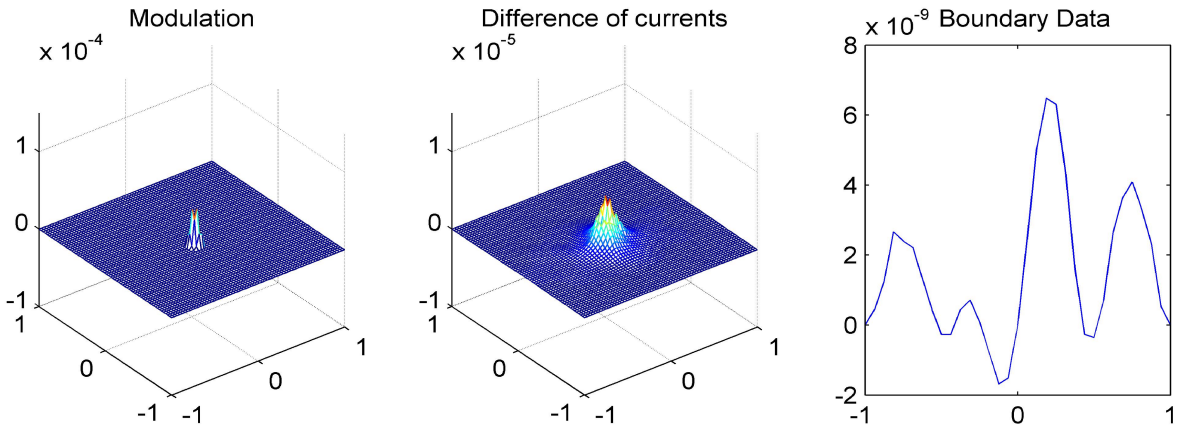

Figure 1.2: Modulation of the conductivity.

information at each point of the domain. Then the second step is to recover some of the electrical properties from this internal data. In the isotropic case the property we aim to recover is the unknown conductivity, in the anisotropic case we consider recovering the current distribution (see last chapter), and in the Maxwell's equations these properties are conductivity, permittivity and permeability.

Chapter 2

ISOTROPIC CASE

2.1 Mathematical model

In this Chapter we study AET (isotropic case) in the existence of only one boundary potential f. We also follow a two step approach. In the first step we propose two separate methods to recover two different internal data, one is $\gamma\nabla u$ (i.e. the current) and the other is an internal data of the form $\gamma^{1/2}\nabla u$. In order to recover $\gamma^{1/2}\nabla u$ we use a set of well chosen test functions and we show that $\gamma^{1/2}\nabla u$ can be recovered by using a fixed boundary potential whose corresponding internal data not necessarily satisfies (2.3). Test functions we used in this step are the traces of special solutions called CGO (Complex Geometrical Optics) solutions. These are defined and discussed in the following sections, and we will mostly follow [43]. The second internal data we recover is the current and in order to recover it we provide an iterative algorithm. In our second step, assuming one of the mentioned internal data is known, we discuss the stability of the recovery of the conductivity, and two Lipschitz type stability estimates are presented (see Theorem 11 and Theorem 14 below). Although the internal data are in different forms the corresponding second steps (the inverse problems with internal data) are similar. We then obtain a uniqueness result (Proposition 10) for AET without assuming any a priori knowledge of the recovered internal data and using one fixed boundary potential.

We first define the inverse problem mathematically. Let Ω be an open bounded connected domain in $\mathbb{R}^n$ with smooth boundary $\partial\Omega$ and γ be the unknown conductivity map whose value is known on the boundary $\partial\Omega$. Throughout this chapter, unless otherwise stated explicitly, we assume that $\gamma \in C^2(\bar{\Omega})$. Let potential u be the solution to the conduc-

tivity equation for a fixed boundary potential $f \in H^{1/2}(\partial\Omega)$. We now define

$$\gamma_m(x) = (1 + m(x))\gamma(x)$$

to be the conductivity after the ultrasound modulation, and we assume that $m \in C^\infty(\bar{\Omega})$ is real valued such that

$$M^{-1} < 1 + m(x) < M, \quad x \in \Omega \tag{2.1}$$

for some $M > 0$. For the sake of simplicity we also assume that M is chosen large enough so that $M^{-1} < \gamma(x) < M$ is satisfied for all $x \in \Omega$. In AET, for some fixed potential $f \in H^{1/2}(\partial\Omega)$, one has the knowledge of the map $M_f(m) : H^{1/2}(\partial\Omega) \to H^{-1/2}(\partial\Omega)$ which is defined by

$$M_f(m) := (\Lambda_{\gamma_m} - \Lambda_\gamma)f \tag{2.2}$$

where m satisfies (2.1). In the physical setting, $M_f(m)$ corresponds to the change in the induced current on the boundary due to the modulation of the conductivity. The inverse problem we are interested in the isotropic case is

Problem 4. *Reconstruction of the conductivity from the knowledge of M_f for a fixed boundary potential f which is imposed on all or some part of the boundary.*

There had been many works on AET. In [3], [4], and [48], as a first step, the internal information $H = \gamma|\nabla u|^2$ in Ω is extracted from the measurements. Here γ is the conductivity and u denotes the voltage potential induced by the boundary potential f. Then assuming $H(x)$ is known for $x \in \Omega$, the AET is reduced to the inverse problem of recovering γ from H. In [48] a stable algorithm to recover the conductivity is given and their method implies the local uniqueness and stability of the reconstruction. AET is also studied in [17] for the 2-dimensional setting under the assumption that the gradient of the potential is bounded away from 0. Then in [5], the authors study the same problem in higher dimensions assuming that one has access to a set of n measurement data corresponding to boundary potentials $\{f_1, \ldots, f_n\}$ and give stability estimates for the inverse problem assuming

$$\det(F_1, \ldots, F_n) \geqslant c_0 > 0. \tag{2.3}$$

In [4] and [48] the AET problem is first converted into an internal data problem where the internal data is $H(x) = \gamma(x)|\nabla u(x)|^2$. The idea of recovering $H(x)$ is as follows. Let's define quadratic form $Q_\gamma(f) = \langle \Lambda_\gamma f, f\rangle$. First observation is that given a smooth bounded function $m(x)$, with the knowledge of M_f one can calculate the derivative of the operator $\gamma \to Q_\gamma$ in the direction of $m(x)$. It is known differentiation is mildly ill-posed but still much better than the ill-posedness of original EIT problem. The Fréchet derivative of $\gamma \to Q_\gamma$ in the direction of $m(x)$ at γ_0 is

$$\mathrm{dQ}_{\gamma_0}(m) : f \mapsto \int_\Omega m(x)\gamma(x)|\nabla u|^2 \,\mathrm{dx} \tag{2.4}$$

where u is the solution to the conductivity equation $\nabla \cdot (\gamma \nabla u) = 0 \,\mathrm{on}\, \Omega$ with $u|_{\partial\Omega} = f$. Note that the value of (2.4) is known for any $m(x)$. As done in [4], by choosing

$$m(x) = \cos(k \cdot x + \varphi)$$

for $\varphi \in \{0, \pi/2\}$ it is possible to recover the Fourier transform of $\gamma(x)|\nabla u|^2$ at any point k and thus the internal data $\gamma|\nabla u|^2$.

In [3], the construction of the internal data $H(x) = \gamma(x)|\nabla u(x)|^2$ is obtained by using focused acoustic waves. They assumed that the ultrasound waves can be focused to a small ball $\omega \subset \Omega$ of volume $|\omega|$. Also another assumption is that γ is known close to the boundary domain in the region

$$\mathrm{dist}(x, \partial\Omega) < d_0$$

where d_0 is very large compared to the radius of ω. Let u_m denote the voltage potential after the ultrasound modulation, so that u_m solves the conductivity equation where conductivity is γ_m. They considered Neumann-to-Dirichlet map instead of Dirichlet-to-Neumann, mathematically they give same information. Thus, in this case the measured response data on the boundary is the potential $(u_m - u)|_{\partial\Omega}$ for any given current ϕ, where

$$\gamma(x)\frac{\partial u_m}{\partial \nu} = \gamma(x)\frac{\partial u}{\partial \nu} = \phi, \mathrm{on}\, \partial\Omega.$$

They showed that one can approximate the internal data $H(x)$ in the order of a power of $|\omega|$. Thus the assumption that the radius of the focal spot ω is crucial for an accurate approximation.

Proposition 5. *([3],Corollary 3.3) Assume that the dimension $d = 2$, that the perturbed area ω is a disk centered at z, and that $u \in W^{2,\infty}(\omega)$. Then, we have*

$$\begin{aligned}\int_\Omega (u_m - u)\phi d\sigma &= \int_\omega \gamma(x)\frac{(\nu(x)-1)^2}{\nu(x)+1}\nabla u \cdot \nabla u \mathrm{d}x + O(|\omega|^{1+\kappa}) \\ &= |\nabla u(z)|^2 \int_\omega \gamma(x)\frac{(\nu(x)-1)^2}{\nu(x)+1}\mathrm{d}x + O(|\omega|^{1+\kappa}).\end{aligned}$$

Therefore, if γ is $C^{0,2\alpha}(\omega)$, with $0 \leqslant \alpha < \kappa \leqslant \frac{1}{2}$, we have

$$\gamma(z)|\nabla u(z)|^2 = S(z) + O(|\omega|^\alpha)(\text{or } o(1) \text{ if } \alpha = 0),$$

where the function $S(z)$ is defined by

$$S(z) = \left(\int_\omega \gamma(x)\frac{(\nu(x)-1)^2}{\nu(x)+1}\mathrm{d}x\right)^{-1} \int_{\partial\Omega} (u_m - u)\phi.$$

Similar to the other hybrid inverse problems AET is converted into an internal data inverse problem where one assumes that $H(x) = \gamma(x)|\nabla u(x)|^2$ is known. Substituting internal data into the conductivity equation gives the following equation

$$\begin{aligned}\nabla \cdot \left(\frac{H(x)}{|\nabla u(x)|^2}u(x)\right) &= 0 \,\text{in}\, \Omega \\ \frac{H(x)}{|\nabla u(x)|^2}\frac{\partial u}{d\nu} &= \phi \,\text{on}\, \partial\Omega. \end{aligned} \tag{2.5}$$

Then in [3], using two distinct boundary currents ϕ_1, ϕ_2 and assuming $\nabla u_1 \times \nabla u_2 \neq 0$ where u_1, u_2 are the solutions corresponding to the boundary data ϕ_1, ϕ_2, respectively, the authors present a reconstruction algorithm for γ by numerical methods.

In [17] for dimension $n = 2$, and in [5] for dimensions $n = 2, 3$, it is shown that the diffusion coefficient γ can be uniquely and stably reconstructed from knowledge of a sufficient large number of power densities of the form $\gamma|\nabla u|^2$. By using a set of internal data $H = \{H_{jk}\}_{jk}$ where $H_{jk} = \gamma \nabla u_j \cdot \nabla u_k$ they write equations for the functions

$S_k = \sqrt{\gamma}\nabla u_k$ that are independent of γ. For a $2D$ setting they consider two 'internal' measurements (H_1, H_2) in $W^{1,\infty}(\Omega)$ corresponding to the boundary potential (g_1, g_2) for conductivity γ. Suppose another conductivity $\tilde{\gamma}$ gives internal data $(\tilde{H}_1, \tilde{H}_2)$ for the same boundary potentials.

Proposition 6. *([5], Theorem 3.2, 2D global uniqueness and stability). Suppose*

$$\det\left(\sqrt{\gamma(x)}\nabla u_1(x), \sqrt{\gamma(x)}\nabla u_2(x)\right) > c_0 > 0, \qquad x \in \Omega \tag{2.6}$$

and $\gamma(x_0) = \tilde{\gamma}(x_0)$ *for some* $x_0 \in \bar{\Omega}$ *then*

$$\|\log\gamma - \log\tilde{\gamma}\|_{W^{1,\infty}(\Omega)} \leqslant C\|H - \tilde{H}\|_{W^{1,\infty}(\Omega)}$$

Here u_1, u_2 are the solutions corresponding to the boundary data g_1, g_2, respectively, and matrices $H, \tilde{H}$ are obtained from the internal data (H_1, H_2) and $(\tilde{H}_1, \tilde{H}_2)$, respectively. In two dimensions, there exists a large class of boundary potentials g such that the crucial constraint (15) above is satisfied over the whole domain Ω (see [2]). They also gave three dimensional version of the above theorem assuming the existence of boundary potentials g_1, g_2, g_3 and corresponding measurements (H_1, H_2, H_3) that satisfy (2.6). However in the three dimensional case, the boundary conditions that satisfy (2.6) is known only for a restrictive class of functions, namely the traces of complex geometrical optics solutions for sufficiently large $|\rho|$. In [9] the authors generalizes these results obtained in [17] and [5] to multi-dimensional case and to internal data of the form

$$\gamma^{\alpha}\nabla u_j \cdot \nabla u_k$$

for arbitrary α.

Another related result is in [4] where the author presents existence, uniqueness, and stability results for the Cauchy problem (2.5). For one measurement data, a local stability estimate and a stable reconstruction (in the sense that the estimate holds only on a part of the boundary holds) is given.

Kuchment and Kunyansky gave a stable local algorithm for the AET problem in [48] (see also [47]). From the formulas they presented the local uniqueness and stability of the reconstruction can be inferred. Their algorithm involves two steps. First, instead of assuming perfectly focused ultrasound modulations they use more realistic spherical waves, and 'synthetically' they recover the perfectly focused data. Second, step of the algorithm is then to recover the unknown conductivity from these perfectly focused perturbations. Their linearized algorithm recovers γ assuming that the conductivity is close to a known one, thus it is a local reconstruction in this sense.

The coupling in the acousto-electric coupling is that the acoustic waves effects or changes the electromagnetic waves. There is a coupling in the converse direction and the imaging technique which makes use of this coupling is called Impedance-Acoustic Tomography which is presented in [25]. Impedance-Acoustic Tomography uses the fact that the absorbed electrical energy inside the body raises its temperature which causes thermal expansion, then this expansion induces acoustic waves as int he case of PAT. These acoustic waves can be measured and recorded outside the body. Then the inverse problem is to calculate the absorbed energy inside the body from these acoustic measurements, and consequently recovering the electrical conductivity. Similar to AET, Impedance-Acoustic Tomography aims to combine the high contrast of EIT with the high resolution of ultrasound.

2.2 Uniqueness

Let $\mu^2 = \gamma \in C^2(\bar{\Omega})$ be the conductivity map as above. Let $u, u_m \in H^1(\Omega)$ be the induced potentials before and after the ultrasound modulation, respectively, that is, u satisfies

$$\begin{aligned} \nabla \cdot (\gamma \nabla u) &= 0, \qquad \text{in } \Omega, \\ u|_{\partial\Omega} &= f, \end{aligned}$$

and u_m satisfies

$$\begin{aligned} \nabla \cdot (\gamma_m \nabla u_m) &= 0, \qquad \text{in } \Omega, \\ u_m|_{\partial\Omega} &= f, \end{aligned}$$

By elliptic regularity ([67]), we have

$$\|u\|_{H^1(\Omega)} \leqslant C_0 \|f\|_{H^{1/2}(\partial\Omega)} = C_f. \tag{2.7}$$

We recall the following elliptic regularity estimate (see for example [22]).

Theorem 7. *Let Ω be a bounded domain with smooth boundary $\partial\Omega$, and γ be as above. Then, for any $f \in H^{1/2}(\partial\Omega)$ the conductivity equation admits a unique solution $u \in H^1(\Omega)$ satisfying*

$$\|u\|_{H^1(\Omega)} \leqslant C \|f\|_{H^{1/2}(\partial\Omega)}$$

where C depends only on Ω and C_0 in (1.1).

When γ is a vector valued function similar estimates still holds. Let $g \in H^{1/2}(\partial\Omega)$. Then, by the divergence theorem

$$\langle M_f(m), g\rangle \;\; = \int_\Omega \gamma_m \nabla u_m \cdot \nabla v_0 - \gamma \nabla u \cdot \nabla v_0 \, \mathrm{d}x \tag{2.8}$$

where $v_0 \in H^1(\Omega)$ is an extension of g to Ω that solves $\nabla \cdot (\gamma \nabla v_0) = 0$. A calculation shows that

$$\begin{aligned} \langle M_f(m), g\rangle \;\; &= \int_\Omega (1+m)\gamma \nabla u_m \cdot \nabla v_0 - \gamma \nabla u \cdot \nabla v_0 \, \mathrm{d}x \\ &= \int_\Omega \gamma(\nabla u_m - \nabla u) \cdot \nabla v_0 \, \mathrm{d}x + \int_\Omega m\gamma \nabla u_m \cdot \nabla v_0 \, \mathrm{d}x. \end{aligned}$$

The first integral of the last equation vanishes taking into account the fact that $u_m - u \in H_0^1(\Omega)$, thus, we obtain

$$\langle M_f(m), g\rangle = \int_\Omega m\gamma \nabla u_m \cdot \nabla v_0 \, \mathrm{d}x. \tag{2.9}$$

Let us write $u_d = u_m - u$. Then $u_d \in H_0^1(\Omega)$, and it solves

$$\nabla \cdot (\gamma_m \nabla u_d) = -\nabla \cdot (m\gamma \nabla u) \text{ in } \Omega, \quad u_d|_{\partial\Omega} = 0.$$

The term $\nabla \cdot (m\gamma \nabla u)$ is bounded in $H^{-1}(\Omega)$, and another application of elliptic regularity shows that

$$\|u_d\|_{H^1(\Omega)} \leqslant K \|m\|_{L^\infty(\Omega)}, \tag{2.10}$$

where K is independent of m. Note that K depends on the L^∞ norm of γ_m which is bounded above by a constant.

Complex Modulations

For the sake of simplicity, we extend the definition of the map M_f to complex modulations. Substituting $u_m = u + u_d$ in (2.9) gives

$$\langle M_f(m), g\rangle \;\; = \int_\Omega m\gamma\nabla u \cdot \nabla v_0 \mathrm{d}x + Q_m(g),$$

where

$$Q_m(g) = \int_\Omega m\gamma\nabla u_d \cdot \nabla v_0 \; \mathrm{d}x.$$

Note that the first term in the decomposition of our measurement operator is linear in m, and the second term is negligible when m is small. Thus, we define M_f for $m(x) = h(x)+in(x)$ as

$$\begin{aligned} \langle M_f(m), g\rangle \;\; &= M_f(h) + iM_f(n) \\ &= \int_\Omega m\gamma\nabla u \cdot \nabla v_0 \mathrm{d}x + R(g) \end{aligned} \tag{2.11}$$

where

$$R(g) := Q_h(g) + iQ_n(g).$$

From (2.10) and the Cauchy-Schwartz inequality we obtain

$$|R(g)| \;\; \leqslant K' \|m\|_{L^\infty(\Omega)} \|m\nabla v_0\|_{L^2(\Omega)}. \tag{2.12}$$

Using CGO solutions to derive the internal data

We now need CGO solutions for the recovery of the internal data. We assume, without losing any generality, that $\bar{\Omega} \subset \{x \in \mathbb{R}^n : x_i > 1, 1 \leqslant i \leqslant n\}$. Fix a vector $\rho \in \mathbb{C}^n$ with $\rho \cdot \rho = 0$ such that $\mathrm{Re}(\rho) \in \{x \in \mathbb{R}^n : x_i \geqslant 0, 1 \leqslant i \leqslant n\}$. Let

$$m(x) = e^{(-\rho - ik)\cdot x}$$

be the ultrasound modulation where $k \in \mathbb{R}^n$ is fixed. Hence,

$$\gamma_m(x) = (1 + e^{(-\rho - ik)\cdot x})\gamma(x)$$

is the modulated conductivity. Note that $\rho \cdot x \geqslant |\rho|$ for $x \in \Omega$, thus the modulation $m(x)$ is small for large $|\rho|$. Let $\mu = \gamma^{-1/2}$. Assuming $|\rho|$ is large enough to satisfy (1.6), choose g so that it is the trace of the CGO solution G for ρ, i.e., $g = G|_{\partial\Omega}$, where

$$G(x) = \mu^{-1}(x)e^{\rho\cdot x}(1 + \psi_\rho(x))$$

with ψ_ρ satisfying estimate (1.8) (see Proposition 2 and following Remark). Then substituting

$$\nabla G = e^{\rho\cdot x}(\mu^{-1}(1 + \psi_\rho)\rho + (1 + \psi_\rho)\nabla\mu^{-1} + \mu^{-1}\nabla\psi_\rho)$$

in (2.11) gives

$$\begin{aligned} \langle M_f(m), g\rangle \quad &= \textstyle\int_\Omega e^{-ik\cdot x}\mu\nabla u \cdot \rho \mathrm{d}x \\ &\quad + \widetilde{O_1}(x) + \widetilde{O_2}(x) + \widetilde{O_3}(x) + R(g) \end{aligned} \tag{2.13}$$

where

$$\begin{aligned} \widetilde{O_1}(x) &= \textstyle\int_\Omega e^{-ik\cdot x}\mu\psi_\rho\nabla u \cdot \rho \mathrm{d}x \\ \widetilde{O_2}(x) &= -\textstyle\int_\Omega e^{-ik\cdot x}(1 + \psi_\rho)\nabla u \cdot \nabla\mu \mathrm{d}x \\ \widetilde{O_3}(x) &= \textstyle\int_\Omega e^{-ik\cdot x}\mu\nabla u \cdot \nabla\psi_\rho \mathrm{d}x \end{aligned}$$

We also assume that $|\rho|$ is sufficiently large so that $e^{-|\rho|} \leqslant |\rho|^{-1}$, and therefore $\|m\|_{L^\infty(\Omega)} \leqslant |\rho|^{-1}$. From this, together with (1.7),(2.7), and (2.12), we can deduce that

$$|\widetilde{O_1}(x)| + |\widetilde{O_2}(x)| + |\widetilde{O_3}(x)| + |R(g)| \leqslant L \tag{2.14}$$

for some L independent of ρ. We define

$$s(k, \rho) = \frac{1}{|\rho|}\langle M_f(m), g\rangle,$$

and from (2.13) we obtain

$$\begin{aligned} s(k, \rho) \quad &= \textstyle\int_\Omega e^{-ik\cdot x}\mu\nabla u \cdot \hat{\rho}\, \mathrm{d}x + O(|\rho|^{-1}). \\ &= (\mu\nabla u.\hat{\rho})\widehat{\ }(k) + O(|\rho|^{-1}). \end{aligned} \tag{2.15}$$

We summarize this result in the following proposition.

Proposition 8. *Suppose we have the knowledge of the map M_f for some fixed $f \in H^{1/2}(\partial\Omega)$. Let u be the solution to the conductivity equation with $u|_{\partial\Omega} = f$. Let $s(k,\rho)$ be defined as above. Then we can recover $F(x) = \mu(x)\nabla u(x)$ by the following formula*

$$\widehat{F}(k) = A^{-1}[(\lim_{\tau\to\infty} s(k,\rho_1)), \ldots, (\lim_{\tau\to\infty} s(k,\rho_n))]^T$$

where $\rho_j = \tau(e_j + ie_n)$ for $1 \leqslant j < n$, $\rho_n = \tau(e_n + ie_1)$, and A is a fixed invertible invertible matrix. Here $\{e_i\}_{i=1}^n$ denotes the standard basis of $\mathbb{R}^n$.

Proof. From (2.15), we already have

$$(\mu\nabla u \cdot \widehat{\rho_j})\widehat{\ }(k) = \lim_{\tau\to\infty} s(k,\rho_j).$$

Then A is the matrix whose k^{th} row is the transpose of the vector $\widehat{\rho_j}$. A is thus invertible with determinant 2. □

Note that the calculation of $s(k,\rho)$ from the map M_f requires the knowledge of traces of CGO solutions. We postpone the discussion of this issue until after having presented the uniqueness result in Section 4.

We now can give a uniqueness result for the AET problem with one boundary potential. The unique determination of the conductivity depends on the fixed boundary potential f. For example, if $f = 0$, then clearly $M_f = M_f'$ for any two distinct conductivities γ and γ'. However, under favorable conditions, this is the only exception to uniqueness. We show that uniqueness holds if $\Lambda_\gamma f$ does not vanish on some (possibly small) part of the boundary $\partial\Omega$. It is known that in dimension $n \geqslant 3$ the knowledge of the Cauchy data on particular subsets of the boundary determines the potential uniquely ([15],[41]). Let $x_1 \in \partial\Omega$ and the tangent plane H of $\partial\Omega$ at x_1 be given. We say that Ω *is strongly star-shaped with respect to* x_1 if every line through x_1 which is not contained in the tangent plane H cuts the boundary $\partial\Omega$ at precisely two distinct points, x_1 and x_2, and the intersection at x_2 is transversal. We use the following result of [41].

Proposition 9. *([41], Corollary 1.4) Let $\gamma, \gamma' \in C^2(\bar{\Omega})$ be strictly positive. Let $\Omega \subset \mathbb{R}^n$ be an open bounded connected set with C^∞ boundary where $n \geqslant 3$. Let x_1 be a point such that the tangent plane H of $\partial\Omega$ at x_1 satisfies $\partial\Omega \cap H = \{x_1\}$. Assume in addition, that Ω is strongly star-shaped with respect to x_1. Assume that $\gamma = \gamma'$ on $\partial\Omega$, and there exists a neighborhood $\omega \in \partial\Omega$ of x_1, such that*

$$\Lambda_\gamma g = \Lambda_{\gamma'} g \ \text{ in}\, \omega, \quad \text{for all}\, g \in H^{1/2}(\partial\Omega). \tag{2.16}$$

Then $\gamma = \gamma'$.

The following is the main result of this section.

Proposition 10. *Let $f \in H^{1+\varepsilon}(\partial\Omega)$ for some $\varepsilon > 0$. Let $\gamma, \gamma', \Omega, x_1$ be as in Proposition 9. Let M_f, M_f' be two maps as defined above for γ and γ', respectively. Assume that $\gamma = \gamma'$ on $\partial\Omega$, and there exists a neighborhood $\omega \in \partial\Omega$ of x_1, such that*

$$\Lambda_\gamma f(x) \neq 0, \quad \text{for}\, a.e.\ x \in \omega$$

Then $M_f = M_f'$ implies $\gamma = \gamma'$.

Proof. If (2.16) holds, then, by Proposition 9 we immediately get $\gamma = \gamma'$. Thus, it remains to show (2.16). Since $C^\infty(\partial\Omega)$ is dense in $H^{1/2}(\partial\Omega)$, and Λ_γ is a bounded operator, it is sufficient to show that (2.16) holds for all $g \in C^\infty(\partial\Omega)$. Let u, u_g be the solutions to (3.1) with boundary data f and g, respectively. The power densities of the form $H(x) = \gamma(x)\nabla u(x) \cdot \nabla u_g(x)$ can be constructed from the knowledge of M_f (see for example [17] or [4] for details). This can be seen by replacing (G, m) with $(u_g, e^{-ik\cdot x})$ in (2.13) and following calculations. Thus,

$$\gamma \nabla u \cdot \nabla u_g = \gamma' \nabla u' \cdot \nabla u_g' \tag{2.17}$$

where u', u_g' are solutions to $\nabla \cdot (\gamma' \nabla v) = 0$ with boundary values $u'|_{\partial\Omega} = f$ and $u_g'|_{\partial\Omega} = g$, respectively. By elliptic regularity, $u, u' \in H^{3/2+\varepsilon}(\Omega)$, and $u_g, u_g' \in C^2(\bar{\Omega})$, thus (2.17) holds in $H^{1/2+\varepsilon}(\Omega)$. Restricting (2.17) to the boundary yields

$$\gamma \partial_\nu u \partial_\nu u_g = \gamma' \partial_\nu u' \partial_\nu u_g'$$

in $L^2(\partial\Omega)$ since the tangential components are equal. Moreover, letting $m = c$ for some constant c gives

$$c\Lambda_\gamma f = M_f(c) = M'_f(c) = c\Lambda_{\gamma'} f.$$

Thus $\gamma\partial_\nu u = \gamma'\partial_\nu u'$ in $L^2(\partial\Omega)$, which in turn implies that $\Lambda_\gamma g(x) = \Lambda_{\gamma'} g(x)$ when $x \notin \{x \in \partial\Omega : \Lambda_\gamma f(x) = 0\}$. In particular, by our assumption on f, for any $h \in H^{1/2}(\partial\Omega) \cap \mathcal{E}'(\omega)$

$$\langle \Lambda_\gamma g, h\rangle = \langle \Lambda_{\gamma'} g, h\rangle,$$

which shows that $\Lambda_\gamma g = \Lambda_{\gamma'} g$ in ω as desired. □

2.3 Stability

In this section, we focus on the inverse problem of recovering the conductivity $\mu^2(x) = \gamma(x)$ from the knowledge of the internal data $\gamma^t(x)\nabla u(x)$, where u solves the conductivity equation with $u|_{\partial\Omega} = f$, and $f \in H^{1/2}(\partial\Omega)$ is a fixed boundary potential. The Lipschitz constants of the stability estimates we present depend on the norms of the coefficients and internal data. For a normed linear space H, we define the generic set of coefficients as

$$\mathcal{B}(M, H) = \{h \in H : \ \|h\|_H \leqslant M\}.$$

We assume that $\mu, \tilde{\mu} \in \mathcal{B}(M, C^2(\bar{\Omega}))$ for some M. We first present the following stability estimate, for the case $t = 1/2$, then we deal with the case of more general t by using an ODE based approach.

Theorem 11. *Let $\mu, \tilde{\mu}, \Omega$ be as above. Let $f, \tilde{f} \in \mathcal{B}(M, H^{1/2}(\partial\Omega))$ be two boundary potentials with corresponding internal data $F = \mu\nabla u$ and $\tilde{F} = \tilde{\mu}\nabla\tilde{u}$, respectively, as above. Then we have the following two stability estimates:*

i. Let $F_{\min}(x) = \min\{|F(x)|^{-1}, |\tilde{F}(x)|^{-1}\}$. If $F_{\min} \in L^2(\Omega)$, then there exists a constant $C = C(M, \Omega)$ such that

$$\|\tilde{\mu} - \mu\|_{L^1(\Omega)} \ \leqslant C\|F_{\min}\|_{L^2(\Omega)}(\|\tilde{F} - F\|_{H^1(\Omega)} + \|\tilde{f} - f\|_{H^{1/2}(\partial\Omega)})$$

ii. Suppose that $\mu, \tilde{\mu} \in \mathcal{B}(M, C^{k,\alpha}(\bar{\Omega}))$, $f, \tilde{f} \in \mathcal{B}(M, C^{k,\alpha}(\partial\Omega))$ *for some* $k \geqslant 1$. *If* $|F(x)| > \delta > 0$, *then there exists a constant* $C = C(M, \Omega)$ *such that*

$$\|\tilde{\mu} - \mu\|_{C^{k-1,\alpha}} \leqslant C(\|\tilde{F} - F\|_{C^{k-1,\alpha}(\bar{\Omega})} + \|\tilde{f} - f\|_{C^{k,\alpha}(\partial\Omega)}).$$

Proof. Our first step is to construct a vector field $J \in L^\infty(\Omega)$ from the internal data F such that u solves

$$\begin{aligned} &\Delta u + J \cdot \nabla u = 0, \text{ on } \Omega \\ &u|_{\partial\Omega} = f. \end{aligned} \tag{2.18}$$

Since u is the solution to the conductivity equation, it satisfies

$$\begin{aligned} 0 &= \mu^{-2}\nabla \cdot \mu^2 \nabla u \\ &= \Delta u + 2\tfrac{\nabla\mu}{\mu} \cdot \nabla u. \end{aligned} \tag{2.19}$$

We cannot calculate the vector field $\frac{\nabla\mu}{\mu}$ directly from the internal data, however, the vector projection of $\frac{\nabla\mu}{\mu}$ onto the vector field ∇u is given by

$$\frac{\nabla\mu \cdot \nabla u}{\mu \nabla u \cdot \nabla u} \nabla u,$$

when $\nabla u \neq 0$ and 0 otherwise. This vector field can be calculated from the internal data by using the fact that

$$\nabla \cdot F = -\nabla\mu \cdot \nabla u,$$

which is a result of (2.19). We thus define

$$J(x) := \frac{-2\nabla \cdot F(x)}{F(x) \cdot F(x)} F(x)$$

on the set $E_0 = \{x \in \Omega : F(x) \neq 0\}$. It is known that the critical set of u has Lebesgue measure 0 ([34]), and J can thus be defined on Ω by the above equality. We obtain the vector field J from the internal data, and moreover

$$J \cdot \nabla u = 2\frac{\nabla\mu}{\mu} \cdot \nabla u. \tag{2.20}$$

Therefore, by (2.19) and (2.20), we conclude that u solves (2.18) on Ω as desired. We now check that J is bounded from above independent of u:

$$\begin{aligned}\left|\frac{-2\nabla\cdot F(x)}{F(x)\cdot F(x)}F(x)\right| &= \left|\frac{2\nabla\mu\cdot\nabla u}{\mu^2\nabla u\cdot\nabla u}\mu\nabla u\right| \\ &\leqslant 2\frac{|\nabla\mu|}{\mu}.\end{aligned}$$

Thus, by the weak maximum principle, the solution w of (2.18) is unique, that is, $w = u$. Similarly, $\tilde{u}$ is the unique solution to (2.18) on Ω with (J, f) replaced by $(\tilde{J}, \tilde{f})$. Let $\Phi = u - \tilde{u}$. Then

$$\begin{aligned}&\Delta\Phi + J\cdot\nabla\Phi = -(J-\tilde{J})\cdot\nabla\tilde{u}, \text{ on}\,\Omega, \\ &\Phi|_{\partial\Omega} = f - \tilde{f}.\end{aligned} \tag{2.21}$$

A calculation shows that

$$\begin{aligned}(J-\widetilde{J})\cdot\nabla\tilde{u} &= \tilde{\mu}^{-1}[(J\cdot F - \widetilde{J}\cdot\tilde{F}) - J\cdot(F-\tilde{F})] \\ &= \tilde{\mu}^{-1}[2(-\nabla\cdot F + \nabla\cdot F) - J\cdot(F-\tilde{F})],\end{aligned} \tag{2.22}$$

which implies

$$\|(J-\widetilde{J})\cdot\nabla\tilde{u}\|_{L^2(\Omega)} \leqslant C\|\tilde{F}-F\|_{H^1(\Omega)}. \tag{2.23}$$

The inequality (2.23) and standard elliptic regularity estimates for the equation (2.21) yield

$$\|u-\widetilde{u}\|_{H^1(\Omega)} \leqslant C(\|\tilde{F}-F\|_{H^1(\Omega)} + \|\tilde{f}-f\|_{H^{1/2}(\partial\Omega)}). \tag{2.24}$$

Note that in the above calculations, we overwrite the definition of constant C (with a greater one whenever needed) for the sake of brevity. Since $\tilde{F} - F = (\tilde{\mu}-\mu)\nabla\tilde{u} + \mu(\nabla\tilde{u} - \nabla u)$, we directly get

$$|\tilde{\mu}(x)-\mu(x)| \leqslant \frac{|\tilde{F}(x)-F(x)| + \mu|\nabla\tilde{u}(x)-\nabla u(x)|}{|\nabla\tilde{u}|}.$$

This calculation is symmetric in the sense that $|\nabla\tilde{u}|$ and $|\nabla u|$ can be permuted. We thus obtain

$$|\tilde{\mu}(x)-\mu(x)| \leqslant \frac{|\tilde{F}(x)-F(x)| + C|\nabla\tilde{u}(x)-\nabla u(x)|}{\max\{|\nabla\tilde{u}(x)|, |\nabla u(x)|\}}, \tag{2.25}$$

which implies

$$\|\tilde{\mu} - \mu\|_{L^1(\Omega)} \leqslant C(\|\tilde{F} - F\|_{L^2(\Omega)} + C\|\tilde{u} - u\|_{H^1(\Omega)})\|F_{\min}\|_{L^2(\Omega)}.$$

Finally, using this inequality and (2.24), the desired result follows immediately.

In order to prove part (ii), we now assume $|F(x)| > \delta > 0$. First note that, by our assumptions and elliptic regularity, we have $F, \tilde{F} \in \mathcal{B}(M', C^{k-1,\alpha}(\bar{\Omega}))$ where M' depends on M and Ω. Then J is also bounded in $C^{k-1,\alpha}(\bar{\Omega})$, and hence (2.22) implies

$$\|(J - \widetilde{J}) \cdot \nabla \tilde{u}\|_{C^{k-2,\alpha}(\bar{\Omega})} \leqslant C\|\tilde{F} - F\|_{C^{k-1,\alpha}(\bar{\Omega})}.$$

Hence, by elliptic regularity applied to the equation (2.21), it follows that

$$\|u - \widetilde{u}\|_{C^{k,\alpha}(\Omega)} \leqslant C(\|\tilde{F} - F\|_{C^{k-1,\alpha}(\bar{\Omega})} + \|\tilde{f} - f\|_{C^{k,\alpha}(\partial\Omega)}). \tag{2.26}$$

Let us write $\tilde{F} - F = (\tilde{\mu} - \mu)\nabla u + \tilde{\mu}(\nabla\tilde{u} - \nabla u)$. Then at any point $x \in \Omega$

$$\tilde{\mu}(x) - \mu(x) = \frac{\mu(x)}{F^2(x)} F(x) \cdot [(\tilde{F}(x) - F(x)) - \tilde{\mu}(x)(\nabla\tilde{u}(x) - \nabla u(x))].$$

By differentiating the last equality, and using the boundedness of $\tilde{\mu}, F, F^{-2}$, and their derivatives, we obtain

$$\|\tilde{\mu} - \mu\|_{C^{k-1,\alpha}} \leqslant C(\|\tilde{F} - F\|_{C^{k-1,\alpha}(\bar{\Omega})} + \|\tilde{u} - u\|_{C^{k,\alpha}(\partial\Omega)}).$$

The desired result now follows from (2.26). □

We additionally note that under weaker regularity conditions than the ones in part (ii) of the above theorem, it is still possible to make similar conclusions. For example, suppose $F_{\min} \in L^\infty(\Omega)$. Then, it can be seen that

$$\|\tilde{\mu} - \mu\|_{L^2(\Omega)} \leqslant C\|F_{\min}\|_{L^\infty(\Omega)}(\|\tilde{F} - F\|_{H^1(\Omega)} + \|\tilde{f} - f\|_{H^{1/2}(\partial\Omega)}),$$

by taking square and integrating both sides of the inequality (2.25).

An ODE based approach

In this part, we use an ODE based method to give a stability estimate assuming a more general internal data of the form $S = \gamma^t \nabla u$ is known for $t \in \mathbb{R}$. In order to achieve this we use two facts, the first is that $\gamma^{-t} S$ is a gradient and second is that $\gamma^{1-t} S$ is a divergence free field. For any vector $\mathrm{v} = (v_1, \ldots, v_n)$ in $\mathbb{R}^n$, let M_{v} denotes the $n \times n$ diagonal matrix whose main diagonal entries are v_i, and let the operator D_{v} be defined as

$$D_{\mathrm{v}} H = \sum_{i=1}^{n} v_i \frac{\partial H_i}{\partial x_i}$$

for any vector field H in $\mathbb{R}^n$. We choose $\mathrm{v} \in \mathbb{R}^n$ such that $D_{\mathrm{v}} \nabla u = 0$. Note that the set of such vectors can be characterized as $\{w\}^{\perp}$ where $w = (1, \ldots, 1)$. Then, when $k \neq 0$ we obtain

$$\begin{aligned} 0 &= D_{\mathrm{v}}(\gamma^{-t} S) \\ &= M_{\mathrm{v}} S \cdot \nabla \gamma^{-t} + (D_{\mathrm{v}} S)\, \gamma^{-t} \\ &= -t M_{\mathrm{v}} S \cdot \nabla \gamma + (D_{\mathrm{v}} S)\, \gamma \end{aligned}$$

for any $\mathrm{v} \in \{w\}^{\perp}$. Note that D_w is the divergence operator, and when $k \neq 1$

$$\begin{aligned} 0 &= D_w(\gamma^{1-t} S) \\ &= (1-t) M_w S \cdot \nabla \gamma + (D_w S)\gamma. \end{aligned}$$

Thus combining last two equalities for any $t \in \mathbb{R}$, we obtain a first order PDE

$$F \cdot \nabla \gamma + H \gamma = 0, \tag{2.27}$$

where F, H and $\mu|_{\partial\Omega}$ are known. Suppose there exists a boundary potential f such that the corresponding coefficient F has integral curves that map any $x \in \Omega$ to a point of boundary in finite time. Then one can transform (2.27) into an ODE by method of characteristics, and solve for $\gamma(x)$ by time reversal. If F is a complex field, then since γ is real, we can obtain two distinct equations by taking real and imaginary parts of the equation (2.27). Thus we

can do similar analysis on any linear combination of these equations. We give the following definition.

Definition 12. *We say a complex vector field F satisfies Property $P_{k,T}$ in Ω, if there exist scalar functions $a, b \in C^k(\bar{\Omega})$ with*

$$\|a\|_{C^k(\bar{\Omega})}, \|b\|_{C^k(\bar{\Omega})} \leqslant 1$$

such that the integral curves of the real vector field $F_{a,b} = a\Re(F) + b\Im(F)$ map a dense subset of Ω to $\partial\Omega$ in time less than T.

Remark. Suppose that γ solves (2.27) for some $F \in C^k(\bar{\Omega})$ and that F satisfies Property $P_{k,T}$, i.e., there are a, b such that $F_{a,b}$ satisfies the property mentioned in the above definition. Then, γ also solves

$$F_{a,b} \cdot \nabla\gamma + H_{a,b}\gamma = 0. \tag{2.28}$$

Moreover,

$$\|F_{a,b} - \tilde{F}_{a,b}\|_{C^k(\bar{\Omega})} \leqslant \|F - \tilde{F}\|_{C^k(\bar{\Omega})}$$

for any $\tilde{F} \in C^k(\bar{\Omega})$, since a and b are bounded in C^k. Thus we don't loose stability when we replace $(F_{a,b}, \tilde{F}_{a,b})$ with $F, \tilde{F}$ since $F \to F_{a,b}$ is a Lipschitz map in $C^k(\bar{\Omega})$.

We give the following lemma for more general coefficients (F, H) than the ones constructed above.

Lemma 13. *Let Ω be a bounded domain with boundary $\partial\Omega$ of class C^{k+1}. Let $F, \tilde{F} \in \mathcal{B}(M, C^k(\bar{\Omega}))$, $H, \tilde{H} \in \mathcal{B}(M, C^{k-1}(\bar{\Omega}))$ given for some $k \geqslant 1$. Suppose F (or $\tilde{F}$) satisfies Property $P_{k,T}$ for some $T > 0$. Let $\gamma \in \mathcal{B}(M, C^k(\bar{\Omega}))$ solves (2.27) and $\tilde{\gamma} \in \mathcal{B}(M, C^k(\bar{\Omega}))$ be the solution of (2.27) corresponding to coefficients $(\tilde{F}, \tilde{H})$. Then for any $\varepsilon > 0$ there exists $C = C(M, \Omega)$ such that*

$$\begin{aligned} \|\gamma - \tilde{\gamma}\|_{C^{k-1}(\Omega)} \leqslant C(&\|\tilde{F} - F\|_{C^{k-1}(\bar{\Omega})} + \|H - \tilde{H}\|_{C^{k-1}(\bar{\Omega})} \\ &+ \left\|\gamma|_{\partial\Omega} - \tilde{\gamma}|_{\partial\Omega}\right\|_{C^{k-1}(\partial\Omega)} + \sup_{|j|<k} \|D^j\gamma - D^j\tilde{\gamma}\|_{C(\Gamma_\varepsilon)}\Big), \end{aligned} \tag{2.29}$$

where $\Gamma_\varepsilon = \{x \in \partial\Omega : |F_{a,b}(x) \cdot \nu(x)| < \varepsilon\}$, and a, b are defined as in Definition 12.

We postpone the proof of the Lemma to the end of this section. We now prove the following stability result.

Theorem 14. *Let Ω be a bounded domain with boundary $\partial\Omega$ of class C^{k+1}. Assume that $\gamma, \tilde{\gamma} \in \mathcal{B}(M, C^k(\bar{\Omega}))$ for $k \geqslant 1$. Let $F, \tilde{F} \in \mathcal{B}(M, C^k(\bar{\Omega}))$ be the corresponding coefficients of (2.27) constructed from boundary potentials $f, \tilde{f} \in \mathcal{B}(M, C^{k+1}(\bar{\Omega}))$, respectively.*

i. Suppose F satisfies Property $P_{k,T}$ for some $T > 0$. Then there is a constant C such that

$$\begin{aligned}\|\gamma - \tilde{\gamma}\|_{C^{k-1}(\Omega)} &\leqslant C(\|\tilde{F} - F\|_{C^k(\bar{\Omega})} + \left\|\gamma|_{\partial\Omega} - \tilde{\gamma}|_{\partial\Omega}\right\|_{C^{k-1}(\partial\Omega)} \\ &\quad + \sup_{|j|<k} \|D^j\gamma - D^j\tilde{\gamma}\|_{C(\Gamma_\varepsilon)}),\end{aligned}$$

where Γ_ε is defined as in Lemma 13.

ii. Suppose f (and therefore F) is real valued such that $|F| > \delta > 0$ in Ω for some δ. Then F satisfies Property $P_{k,T}$ for some $T > 0$

iii. There is an open set of boundary potentials $f \in C^{k,\alpha}(\partial\Omega)$ such that the recovered internal data satisfies Property $P_{k,T}$.

Remark. The stability estimate in (i) requires that we need to control not only tangential but also the normal derivatives of $\gamma - \tilde{\gamma}$ in order to have a higher order control on $\gamma - \tilde{\gamma}$. However, if we additionally assume that $|F_{a,b}(x)| > \delta > 0$ for $x \in \partial\Omega$, then by modifying the proof of part (ii) of Theorem 11 by using Schauder type estimates near boundary, it is possible to bound the normal derivatives of $\gamma - \tilde{\gamma}$ at the boundary. Combining this assumption with the above result thus gives a stability estimate involving only tangential derivatives.

Proof. (of Theorem 14) As noted above, $\gamma \in C^k(\bar{\Omega})$ solves (2.27), and $\tilde{\gamma} \in C^k(\bar{\Omega})$ is the solution of (2.27) with coefficients $(\tilde{F}, \tilde{H})$. Let $a, b \in C^k(\bar{\Omega})$ be defined as in Definition 12. Thus γ solves (2.28), and similarly $\tilde{\gamma}$ solves

$$\tilde{F}_{a,b} \cdot \nabla\tilde{\gamma} + \tilde{H}_{a,b}\tilde{\gamma} = 0.$$

Since $F \to F_{a,b}$ is a Lipschitz map in $C^k(\bar{\Omega})$, $\|H_{a,b} - \tilde{H}_{a,b}\|_{C^{k-1}(\bar{\Omega})}$ is bounded above by $\|H - \tilde{H}\|_{C^{k-1}(\bar{\Omega})}$, and thus bounded by $\|\tilde{F} - F\|_{C^k(\bar{\Omega})}$. The stability estimate in (i) now follows from Lemma 13.

Next, we show that F satisfies Property $P_{k,T}$ for some $T > 0$ assuming F is real and $|F| > \delta > 0$ in Ω. This can be seen from the fact that the velocity vector along the integral curve is parallel to ∇u, but u is bounded above by the maximum principle. More precisely, let $\varphi(x_0, t)$ be the integral curve of F starting at x_0. Existence and uniqueness of φ is guaranteed by Picard-Lindelöf theorem, since F Lipschitz. Then,

$$\begin{aligned} \int_0^t \gamma^{-1}(\varphi(x_0,s))F^2(\varphi(x_0,s))\mathrm{d}t &= \int_0^t \dot{\varphi}(x_0,s)\cdot\nabla u(\varphi(x_0,s))\mathrm{d}s \\ &= u(\varphi(x_0,t)) - u(x_0). \end{aligned}$$

The value of the integral on the left hand side is bounded below by $\|\gamma\|^{-1}_{L^\infty(\Omega)}\delta^2 t$, and increases as t increases. However, the right hand side is bounded above independent of x_0 and t. We thus conclude that there exists a time T such that any integral curve exits Ω in a time less than T. This proves (ii).

We now use CGO solutions in order to show the existence of the open set mentioned in (iii). We follow similar steps as in [11]. Fix $\rho \in \mathbb{C}^n$ such that $\rho \cdot \rho = 0$ with $|\rho|$ sufficiently large (to be defined precisely below). Let $s = \frac{n}{2} + k + \varepsilon$. Suppose $\gamma \in H^{s+2}(\Omega)$. Then by Proposition 2 and the remark following it, there exists a solution $u = \gamma^{-1}e^{\rho\cdot x}(1 + \psi_\rho)$ with

$$|\rho|\|\psi_\rho\|_{C^k(\bar{\Omega})} + \|\psi_\rho\|_{C^{k+1}(\bar{\Omega})} \leqslant C$$

for some C independent of ρ. Let $f = u|_{\partial\Omega}$. Then a calculation shows that

$$F = A_t\gamma^t\nabla u = \gamma^{t-1/2}e^{\rho\cdot x}A_t(\rho + R(x))$$

such that $\|R\|_{C^k(\bar{\Omega})}$ is bounded from above independent of ρ. Let $\rho = \xi + i\eta$. Define $a, b \in C^\infty(\bar{\Omega})$ as

$$a(x) + ib(x) = |\rho|^{-k}e^{i\eta\cdot x}$$

so that $\|a\|_{C^k(\bar{\Omega})}$,$\|b\|_{C^k(\bar{\Omega})} \leqslant 1$. We note that $F_{\alpha a,\alpha b} = \alpha F_{a,b}$, and for any scalar h

$$(hF)_{\Re(h),\Im(h)} = |h(x)|^2\, \Re(F(x)).$$

We then get

$$\begin{aligned} F_{a,b} &= \gamma^{t-1/2}|\rho|^{-k} e^{\xi\cdot x} A_t \Re(\rho + R(x)) \\ &= \gamma^{t-1/2}|\rho|^{-k} e^{\xi\cdot x} A_t(\xi + r(x)), \end{aligned}$$

where $r(x) = \Re(R(x))$. Since $\|r\|_{C^k(\bar{\Omega})}$ is bounded independent of $|\rho|$, we can fix $|\rho| = \sqrt{2}|\xi|$ sufficiently large so that $|\xi| > 2\|r(x)\|_{C(\bar{\Omega})}$. Then by Cauchy-Schwartz

$$|\hat{\xi}\cdot F_{a,b}| \;\geqslant C|\rho|^{-k} e^{\xi\cdot x\frac{|\xi|}{2}}$$

for some positive constant C. Since Ω is bounded, $|\hat{\xi}\cdot F_{a,b}| > \delta$ for some $\delta > 0$, thus the integral curves of $F_{a,b}$ maps any point $x \in \Omega$ to boundary in time less than $\operatorname{diam}(\Omega)/\delta$. This shows that the coefficient F corresponding to the boundary potential $f = u|_{\partial\Omega}$ satisfies Property $P_{k,T}$ for some $T > 0$. By elliptic regularity, the vector field $\gamma^k \nabla u$ is stable under the perturbation (in $C^{k,\alpha}(\partial\Omega)$) of f. As noted above $F \mapsto F_{a,b}$ is also stable, thus the above arguments can be applied for boundary potentials near f in $C^{k,\alpha}(\partial\Omega)$ norm. □

We conclude this section with the proof of the lemma.

Proof. (of Lemma 13) First note that, we can assume without losing generality that F is a real vector field. We can make this assumption by considering $F_{a,b}$ and $\tilde{F}_{a,b}$ instead of F and $\tilde{F}$, respectively, and by recalling Definition 12 and the remark following it. Since F is of class C^1, it is Lipschitz continuous in Ω. Thus by Picard-Lindelöf theorem there exists a unique integral curve $\varphi_{x_0}(t) = \varphi(x_0, t)$ of the vector field F starting at $x_0 \in \Omega$, that is,

$$\dot{\varphi}(x_0, t) = F(\varphi(x_0, t)), \quad \varphi(x_0, 0) = x_0.$$

Similarly, we define $\widetilde{\varphi}(x_0, t)$ to be the integral curve of $\tilde{F}$ starting at $x_0 \in \Omega$. Then

$$\dot{\tilde{\varphi}}(x_0, t) - \dot{\varphi}(x_0, t) = \tilde{F}(\tilde{\varphi}(x_0, t)) - F(\varphi(x_0, t)). \tag{2.30}$$

Both F and $\tilde{F}$ are Lipschitz, thus, assuming both integral curves stay in Ω at time t, an application of Grönwall's lemma yields

$$|\tilde{\varphi}(x_0,t)-\varphi(x_0,t)| \leqslant Ct\|\tilde{F}-F\|_{C(\bar{\Omega})},$$

for some constant C depending on the Lipschitz constants of F and $\tilde{F}$. We now assume that $x_0 \in \Omega$ is an element of the dense set mentioned in the Definition 12, i.e., the flow line $\varphi(x_0,\cdot)$ hits the boundary for the first time at $T_{x_0} < T$, thus

$$|\tilde{\varphi}(x_0,t)-\varphi(x_0,t)| \leqslant CT\|\tilde{F}-F\|_{C(\bar{\Omega})},$$

for $0 \leqslant t \leqslant \min\{T_{x_0},\tilde{T}_{x_0}\}$. Moreover, both φ and $\tilde{\varphi}$ are of class C^k. Then taking spatial partial derivatives of (2.30) and using the fact that $D^\alpha F$ is Lipschitz for any multi-index α with $|\alpha| \leqslant k-1$, we can obtain

$$|D^\alpha[\tilde{\varphi}(x,t)-\varphi(x,t)]| \leqslant C'\|\tilde{F}-F\|_{C^{k-1}(\bar{\Omega})} \tag{2.31}$$

by using similar arguments as above. For more details, we refer the reader to [20] or [11] where the estimate (2.31) is established. We now fix $\tau < \min\{T_{x_0},\tilde{T}_{x_0}\}$. Restricting of (2.27) to the curves φ and $\tilde{\varphi}$ gives two equations, and by time reversal we obtain the following ODE's

$$\begin{aligned} -\tfrac{\mathrm{d}}{\mathrm{d}t}\gamma(\psi(t))+H(\psi(t))\gamma(\psi(t))=0, \qquad & -\tfrac{\mathrm{d}}{\mathrm{d}t}\tilde{\gamma}(\tilde{\psi}(t))+\tilde{H}(\tilde{\psi}(t))\tilde{\gamma}(\tilde{\psi}(t))=0,\\ \gamma(\psi(0))=\gamma(\varphi(x_0,\tau)), \qquad & \tilde{\gamma}(\tilde{\psi}(0))=\tilde{\gamma}(\tilde{\varphi}(x_0,\tau)), \end{aligned}$$

where $\psi(t)=\varphi(x_0,\tau-t)$ and $\tilde{\psi}(t)=\tilde{\varphi}(x_0,\tau-t)$ for $t\in[0,\tau]$. More generally, if the integral curves of F map $x\in\Omega$ to the boundary in time $T_x<T$, then

$$\gamma(x)=\gamma(\varphi(x,\tau))e^{\int_0^\tau H(\varphi(x,s))\mathrm{d}s}, \quad \text{and} \quad \tilde{\gamma}(x)=\tilde{\gamma}(\tilde{\varphi}(x,\tau))e^{\int_0^\tau \tilde{H}(\tilde{\varphi}(x,s))\mathrm{d}s}. \tag{2.32}$$

These solutions are obtained by solving the above two ODE's, and evaluating them at $t=\tau$. The functions $\gamma(\varphi(x,\tau))$ and $e^{\int_0^\tau H(\varphi(x,s))\mathrm{d}s}$ are bounded in $C^{k-1}(\bar{\Omega})$, thus by the chain and product rules, the stability of γ (at point x) reduces to the stability of the functions

$\gamma(\varphi(\cdot,\tau))$ and $\int_0^\tau H(\varphi(\cdot,s))\mathrm{d}s$. Let D^α denotes the spatial partial derivation operator for a multi-index α. Then, for any α with $|\alpha| \leqslant k-1$, a calculation shows that

$$\begin{aligned}\left|D^\alpha[\gamma(\varphi(x,\tau)) - \tilde{\gamma}(\tilde{\varphi}(x,\tau))]\right| \quad &\leqslant C\left(\|\varphi(\cdot,\tau) - \tilde{\varphi}(\cdot,\tau)\|_{C^{k-1}(\bar{\Omega})}\right. \\ &\left. + \sup_{|j|\leqslant|k-1|}\left|D^j\gamma|_{x_\tau} - D^j\tilde{\gamma}|_{\tilde{x}_\tau}\right|\right),\end{aligned} \tag{2.33}$$

where $x_\tau = \varphi(x,\tau)$ and $\tilde{x}_\tau = \tilde{\varphi}(x,\tau)$. In obtaining the above inequality, we used the fact that $D^j\gamma$ and $D^j\tilde{\gamma}$ are both continuously differentiable and thus Lipschitz on $\bar{\Omega}$. Then by (2.31)

$$\begin{aligned}\left|D^\alpha[\gamma(\varphi(x,t)) - \tilde{\gamma}(\tilde{\varphi}(x,t))]\right| \quad &\leqslant C'(\|\tilde{F} - F\|_{C^{k-1}(\bar{\Omega})} \\ &+ \sup_{|j|\leqslant|k-1|}\left|D^j\gamma|_{x_\tau} - D^j\tilde{\gamma}|_{\tilde{x}_\tau}\right|).\end{aligned} \tag{2.34}$$

It remains to show a similar stability estimate for $x \mapsto \int_0^\tau H(\varphi(x,s))\mathrm{d}s$. Since $\tau \leqslant T$, differentiation under the integral sign can be justified. Thus by (2.31), for any multi-index α with $|\alpha| \leqslant k-1$, we have

$$\begin{aligned}\left|D^\alpha\textstyle\int_0^\tau H(\varphi(x,s)) - \tilde{H}(\tilde{\varphi}(x,s))\mathrm{d}s\right| \quad &\leqslant C(\|H - \tilde{H}\|_{C^{k-1}(\bar{\Omega})} \\ &+ \|\tilde{F} - F\|_{C^{k-1}(\bar{\Omega})}).\end{aligned} \tag{2.35}$$

where C depends on T, k, and the norms of $H, \tilde{H}, F, \tilde{F}$, but not on x. Let $\omega = T_x = \min\{T_x, \tilde{T}_x\}$. By our assumption, we know that $\omega < T$. Thus, by (2.32), (2.34), (2.35), and letting $\tau \to \omega$, we obtain

$$\begin{aligned}\left|D^\alpha[\gamma(x) - \tilde{\gamma}(x)]\right| \quad &\leqslant C'(\|\tilde{F} - F\|_{C^{k-1}(\Omega)} + \|H - \tilde{H}\|_{C^{k-1}(\bar{\Omega})} \\ &+ \sup_{|j|\leqslant|k-1|}\left|D^j\gamma|_{x_\omega} - D^j\tilde{\gamma}|_{\tilde{x}_\omega}\right|).\end{aligned}$$

$D^j\tilde{\gamma}$ is Lipschitz for $|j| \leqslant k-1$, thus,

$$|D^j\tilde{\gamma}|_{x_\omega} - D^j\tilde{\gamma}|_{\tilde{x}_\omega}| \leqslant \|\tilde{\gamma}\|_{C^k(\bar{\Omega})}|x_\omega - \tilde{x}_\omega| \leqslant CT\|\tilde{F} - F\|_{C(\bar{\Omega})}.$$

Since $x_\omega \in \partial\Omega$, by triangular inequality, we obtain

$$\begin{aligned}\left|D^\alpha[\gamma(x) - \tilde{\gamma}(x)]\right| \quad &\leqslant C(\|\tilde{F} - F\|_{C^{k-1}(\bar{\Omega})} + \|H - \tilde{H}\|_{C^{k-1}(\bar{\Omega})} \\ &+ \sup_{|j|<k}\|D^j\gamma - D^j\tilde{\gamma}\|_{C(\partial\Omega)}).\end{aligned}$$

We note that this inequality is point-wise, and holds for any x such that the integral curves of F map $x \in \Omega$ to the boundary in time less than T. But by our assumption on the vector field F, the collection of such points are dense in Ω. Thus, continuity of $D^\alpha(\gamma - \tilde{\gamma})$ yields

$$\begin{aligned} \|\gamma - \tilde{\gamma}\|_{C^{k-1}(\Omega)} &\leqslant C(\|\tilde{F} - F\|_{C^{k-1}(\bar{\Omega})} + \|H - \tilde{H}\|_{C^{k-1}(\bar{\Omega})} \\ &\quad + \sup_{|j|<k} \|D^j\gamma - D^j\tilde{\gamma}\|_{C(\partial\Omega)}). \end{aligned} \tag{2.36}$$

In order to obtain (2.29) from (2.36), we decompose Ω into two components $\Omega_\varepsilon, \Omega_0$ where

$$\Omega_\varepsilon = \{x \in \Omega : \varphi(x, T_x) \in \Gamma_\varepsilon\},$$

and $\Omega_0 = \Omega \setminus \Omega_\varepsilon$. We recall that $\varphi(x, T_x)$ denotes the first hitting point on $\partial\Omega$ of the flow line starting at $x \in \Omega$. It remains to give a stronger estimate when $x \in \Omega_0$, i.e., with a bound depending only on tangential derivatives of $(\gamma - \tilde{\gamma})$. From (2.27), we calculate

$$(\nabla\gamma - \nabla\tilde{\gamma}) \cdot F = -(H - \tilde{H})\gamma - (\gamma - \tilde{\gamma})\tilde{H} - (F - \tilde{F}) \cdot \nabla\tilde{\gamma}. \tag{2.37}$$

Let $\Gamma_0 = \partial\Omega \setminus \Gamma_\varepsilon$. We fix $x_1 \in \Gamma_0$, so that $|F_\nu(x_1)| = |F(x_1) \cdot \nu(x_1)| \geqslant \varepsilon$. We also note that

$$\begin{aligned} \big|(\partial_\nu\gamma(x_1) - \partial_\nu\tilde{\gamma}(x_1))F_\nu(x_1)\big| &\leqslant \big|\big(\nabla\gamma(x_1) - \nabla\tilde{\gamma}(x_1)\big) \cdot F(x_1)\big| \\ &\quad C' \left\|\gamma|_{\partial\Omega} - \tilde{\gamma}|_{\partial\Omega}\right\|_{C^1(\partial\Omega)}, \end{aligned}$$

for some C' depending on F. Thus considering the equality (2.37) at x_1 yields

$$\begin{aligned} \big|(\partial_\nu\gamma(x_1) - \partial_\nu\tilde{\gamma}(x_1))F_\nu(x_1)\big| &\leqslant C(\|\tilde{F} - F\|_{C(\bar{\Omega})} + \|H - \tilde{H}\|_{C(\bar{\Omega})} \\ &\quad + \left\|\gamma|_{\partial\Omega} - \tilde{\gamma}|_{\partial\Omega}\right\|_{C^1(\partial\Omega)}\Big). \end{aligned}$$

This holds for any $x_1 \in \Gamma_0$, and since $|F_\nu(x_1)| \geqslant \varepsilon$ we obtain

$$\begin{aligned} \sup_{|j|\leqslant 1} \|D^j\gamma - D^j\tilde{\gamma}\|_{C(\Gamma_0)} &\leqslant C(\|\tilde{F} - F\|_{C(\bar{\Omega})} + \|H - \tilde{H}\|_{C(\bar{\Omega})} \\ &\quad + \left\|\gamma|_{\partial\Omega} - \tilde{\gamma}|_{\partial\Omega}\right\|_{C^1(\partial\Omega)}\Big). \end{aligned}$$

The higher order estimates can be established in a similar way. By differentiating (2.37), and using an induction argument, it can be seen that

$$\begin{aligned} \sup_{|j|<k} \|D^j\gamma - D^j\tilde{\gamma}\|_{C(\Gamma_0)} &\leqslant C(\|\tilde{F} - F\|_{C^{k-2}(\bar{\Omega})} + \|H - \tilde{H}\|_{C^{k-2}(\bar{\Omega})} \\ &\quad + \left\|\gamma|_{\partial\Omega} - \tilde{\gamma}|_{\partial\Omega}\right\|_{C^{k-1}(\partial\Omega)}\Big). \end{aligned}$$

Combining this with (2.36) establishes (2.29). □

2.4 Construction and Numerical results

In order to give an approximation to the current $J(x) = \gamma(x)\nabla u(x)$ induced by the boundary potential f, let us set the modulation function as

$$m_z(x) = \varepsilon m(x - z)$$

where m is a nonnegative smooth function supported in a ball of radius r about 0 and bounded by 1 with $\int m = 1$. We also require that r is comparable to ε, that is there exists a positive constant c such that $c^{-1}\varepsilon < r < c\varepsilon$. We now explain our linearization procedure. We first fix z and note that all the integrations and norms below are in x variable. Then

$$\langle M_f(m_z), g\rangle \;=\; \int_\Omega m_z\gamma\nabla u\cdot\nabla G\mathrm{d}x + \int_\Omega \gamma_{m_z}\nabla u_d\cdot\nabla G\mathrm{d}x \tag{2.38}$$

where $u_d = u_{m_z} - u$, and G is any harmonic extension of g to Ω. We emphasize that this time we don't require G to be a solution to the conductivity equation. Clearly u_d depends on z and it is the solution of

$$\nabla\cdot(\gamma\nabla u_d) = -\nabla m_z\cdot J \quad \text{in}\,\Omega, \qquad u_d|_{\partial\Omega} = 0. \tag{2.39}$$

Let u_d' be the solution to

$$\nabla\cdot(\gamma\nabla u_d') = -\nabla m_z\cdot J(z) \quad \text{in}\,\Omega, \qquad u_d'|_{\partial\Omega} = 0, \tag{2.40}$$

For the sake of brevity we define $J_z = J(z)$, and let $(J_z)_i$ denote the i^{th} component of J_z, then we can decompose u_d' as

$$u_d'(x) = \sum_{i=1}^{n}(J_z)_i u_d^i(x)$$

where each u_d^i solves

$$\begin{aligned}\nabla\cdot(\gamma\nabla u_d^i) &= -(\nabla m_z)_i, \qquad \text{in}\,\Omega\\ u_d^i &= 0, \qquad \text{on}\,\partial\Omega\end{aligned}$$

for $1 \leqslant i \leqslant n$. We now write u_d^i as

$$u_d^i = \varepsilon \left(\frac{w_i}{\gamma} + h_i + r_i \right),$$

then the last PDE can be written as the following system of elliptic PDE's

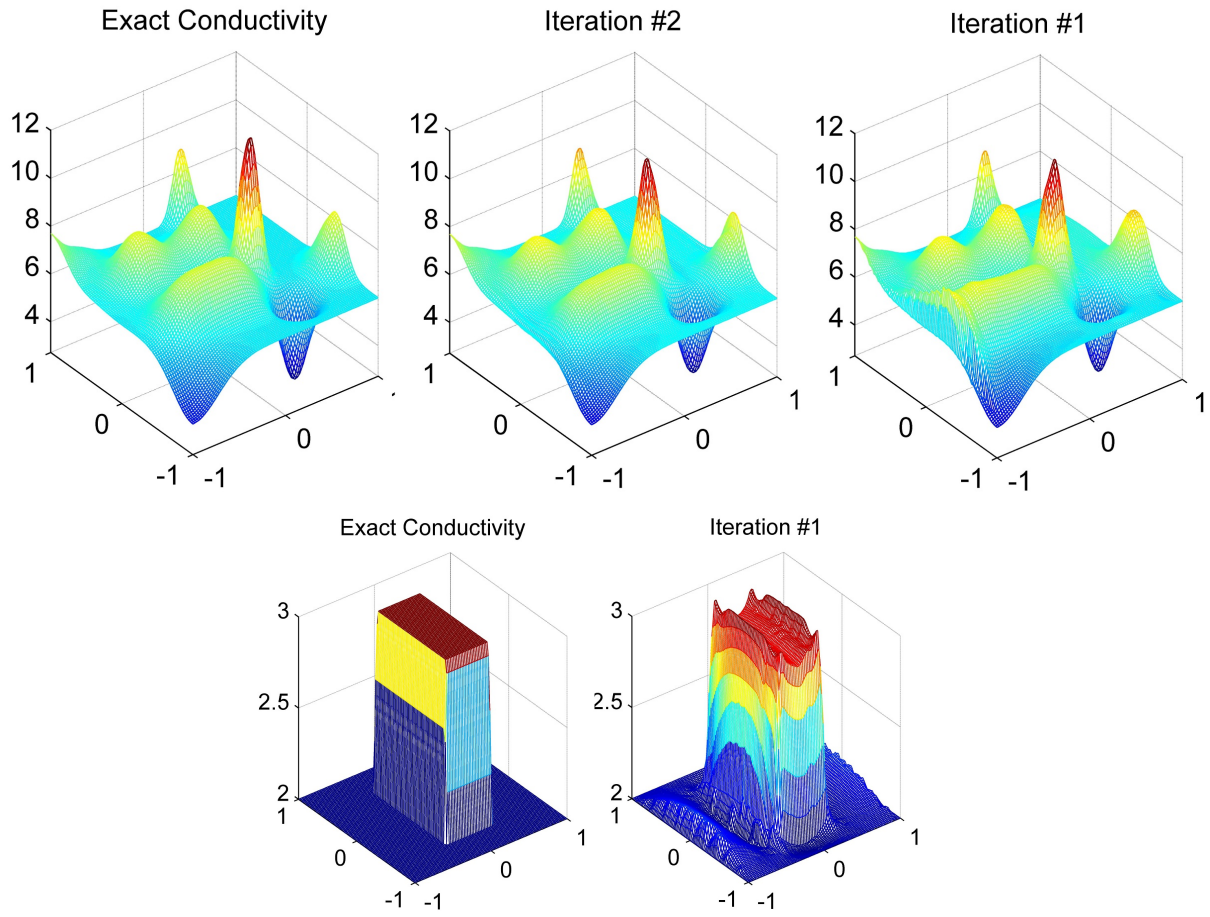

Figure 2.1: Two conductivity distributions with different properties are tested. Mesh size is 64x64 in both cases.

$$\begin{aligned} \Delta w_i(x) &= -(\nabla m(x-z))_i, \\ \nabla \cdot (\gamma(x) \nabla h_i(x)) &= 0, \\ \nabla \cdot (\gamma(x) \nabla r_i(x)) &= \nabla \cdot \left(w_i(x) \tfrac{\nabla \gamma(x)}{\gamma(x)} \right), \end{aligned} \tag{2.41}$$

in Ω and we choose the boundary conditions as

$$\begin{aligned} w_i &= 0, \quad \text{on } \partial\Omega \\ h_i &= -r_i, \quad \text{on } \partial\Omega \\ \partial_\nu r_i &= 0, \quad \text{on } \partial\Omega. \end{aligned} \tag{2.42}$$

These solutions will be our main objects of the reconstruction algorithm. We note that one can calculate w_i directly since the modulation m_z is known. Now our next step is to estimate the last term of (2.38). We have

$$\begin{aligned} \int_\Omega \gamma \nabla u_d^i \cdot \nabla G &= \varepsilon \int_\Omega \gamma \nabla(\gamma^{-1} w_i + h_i + r_i) \cdot \nabla G \mathrm{d}x \\ &= \varepsilon \int_\Omega (\nabla w_i + \gamma \nabla h_i) \cdot \nabla G \mathrm{d}x + \varepsilon \int_\Omega (\gamma \nabla r_i - w_i \gamma^{-1} \nabla \gamma) \cdot \nabla G \mathrm{d}x \\ &= \varepsilon \int_\Omega \nabla \cdot (w_i \nabla G) \mathrm{d}x + \varepsilon \int_\Omega \nabla \cdot (\gamma \nabla h_i G) \mathrm{d}x \\ &= -\varepsilon \langle \Lambda_\gamma(r_i|_{\partial\Omega}), G \rangle \end{aligned}$$

from the divergence theorem and the definitions of $w_i, h_i,$ and r_i. Combining this with (2.38) we obtain

$$\begin{aligned} \langle M_f(m_z), g \rangle &= \int_\Omega m_z \gamma \nabla u \cdot \nabla G \mathrm{d}x + \int_\Omega \gamma_{m_z} \nabla u_d \nabla G \mathrm{d}x \\ &= \int_\Omega m_z \gamma \nabla u \cdot \nabla G \mathrm{d}x + \varepsilon \int_\Omega \gamma_{m_z} \nabla u_d' \nabla G \mathrm{d}x + Q_1(z) \\ &= \int_\Omega m_z \gamma \nabla u \cdot \nabla G \mathrm{d}x - \varepsilon \sum_{i=1}^n (J_z)_i \langle \Lambda_\gamma(r_i|_{\partial\Omega}), G \rangle + Q_1(z) + Q_2(z) \end{aligned}$$

where Q_1, Q_2 represents the error in the above linearization and given by

$$\begin{aligned} Q_1(z) &= \textstyle\int_\Omega \gamma_{m_z} \nabla(u_d - u_d') \nabla G \mathrm{d}x, \\ Q_2(z) &= \textstyle\int_\Omega m_z \gamma \nabla u_d' \nabla G \mathrm{d}x. \end{aligned}$$

If we assume that J is a Lipschitz on Ω with Lipschitz constant L then we can estimate $u_d - u_d'$ by standard elliptic regularity

$$\|u_d - u_d'\|_{H^1(\Omega)} \leqslant rL \|m_z\|_{L^2(\Omega)}$$

and it is straightforward to show that

$$Q_1(z) + Q_2(z) = O(\varepsilon^2 \|\nabla G\|_{L^2(\Omega)}).$$

Thus we obtain

$$\begin{aligned} \langle M_f(m_z), g\rangle &= \varepsilon J(z) \cdot \left(\int_\Omega m(x-z)\nabla G(x)\mathrm{d}x - \langle \Lambda_\gamma(r|_{\partial\Omega}), G\rangle\right) \\ &\quad + O(\varepsilon^2 \|\nabla G\|_{L^2(\Omega)}) \end{aligned}$$

Here by $\langle \Lambda_\gamma(r|_{\partial\Omega}), G\rangle$ we mean the vector valued function $\sum_{i=1}^n e_i \langle \Lambda_\gamma(r_i|_{\partial\Omega}), G\rangle$. Now we have freedom to choose the test function $g = G|_{\partial\Omega}$ and we let $G(x) = x_i$. We get

$$\langle M_f(m_z), x_i\rangle = \varepsilon \left((J_z)_i \int_\Omega m(x-z)\mathrm{d}x - \langle \Lambda_\gamma(r|_{\partial\Omega}), x_i\rangle \cdot J_z\right) + O(\varepsilon^2).$$

Then

$$K(z) = (I + R[\gamma](z))J(z) + O(\varepsilon), \tag{2.43}$$

where I denotes the identity matrix, $K(z)$ can be directly calculated from the measurements

$$K(z) := \sum_{i=1}^n \varepsilon^{-1} \langle M_f(m_z), x_i\rangle e_i, \tag{2.44}$$

and R denotes the matrix valued operator such that

$$(R[\gamma])_{j,i} := \langle \Lambda_\gamma(r_i|_{\partial\Omega}), x_j\rangle.$$

where r_i solves (2.41) with boundary conditions (2.42). $R[\gamma]$ can be estimated by $\|\gamma^{-1}\nabla\gamma\|_{L^2(\Omega)}$ thus the matrix $(I + R[\gamma])$ is invertible at each z if we assume that $\|\gamma^{-1}\nabla\gamma\|_{L^2(\Omega)}$ is small. Next we discuss the recovery of γ from J, thus (2.43) allows an iterative algorithm to construct γ and this is discussed in the last part of this section along with some numerical examples.

The construction procedure of the internal data $F(x)$ requires to test the functional $M_f(m)$ against the traces of CGO solutions which are not known. In order to obtain the internal data $F = \mu\nabla u$ by using CGO solutions one needs high precision in the computation of M_f. Note that the proof of Proposition 10 shows that the knowledge of M_f implies

the knowledge of Λ_γ under certain conditions. More precisely, assume the hypotheses of Proposition 10, and in addition assume that the set

$$\mathcal{N} = \{x \in \partial\Omega : \ \Lambda_\gamma f(x) = 0\}$$

has measure 0 in $\partial\Omega$. Then, following the steps of the proof, it is possible to obtain $\Lambda_\gamma g$ for all $g \in H^{1/2}(\partial\Omega)$. Moreover from a practical point of view, it is not unreasonable to assume we have access to Λ_γ since the calculation of M_f already requires the knowledge of Λ_γ. Assuming we have access to Λ_γ, it is possible to construct the traces of CGO solutions ([53]) also traces of CGO solutions have been computed numerically in [42]. However the method presented in Section 3 implies that when higher accuracy is needed one needs to use larger $|\rho|$. Unfortunately such test functions are not physical and the construction procedure given in Section 3 to recover $\sqrt{\gamma}\nabla u$ becomes numerically unstable when $|\rho|$ is large.

We now give a proposal of an algorithm to recover γ and the current $\gamma\nabla u$ that uses physical test functions. We start with an initial conductivity guess γ_0 and calculate

$$(R[\gamma])_{j,i} := \langle \Lambda_\gamma(s_i|_{\partial\Omega}), x_j \rangle$$

where s_i is the solution to

$$\nabla \cdot (\gamma_0(x)\nabla s_i(x)) \ = \ \nabla \cdot \left(w_i(x) \tfrac{\nabla\gamma_0(x)}{\gamma_0(x)} \right), \tag{2.45}$$

and w_i is defined as in (2.41) and (2.42). We assume $\|\gamma_0^{-1}\nabla\gamma_0\|_{L^2(\Omega)}$ is small so that $(I + R[\gamma_0])$ is invertible so that we can calculate

$$J_0(z) \ := \ (I + R[\gamma](z))^{-1} K(z) \tag{2.46}$$

where $K(z)$ is defined as in (2.44).

By using (2.46), we now have an estimate for the current in domain Ω. Then by using the ODE method (described in the proofs of Lemma 13 and Theorem 14), we recover our first estimate γ_1 to the conductivity from the knowledge of current estimation J_0. We

then update the conductivity in (2.45) in order to proceed to the next iteration. In fact in the numerical examples that are presented in this section, we started the iteration with a constant conductivity (that is the first estimate of the current is $J_0(z) = K(z)$) and the first iterations are still providing good approximations to the conductivity (see Figure 2.1). We note that it is also possible to change this algorithm so that it works without assuming the knowledge of Λ_γ, in that case one needs to estimate $\langle \Lambda_\gamma(s_i|_{\partial\Omega}), x_j \rangle$ by using the conductivity estimate of the algorithm. The equations given in (2.41) and (2.42) have a smoothing effect on the reconstruction. In fact, it can be seen from the numerical examples that even when $\|\gamma^{-1}\nabla\gamma\|_{L^2(\Omega)}$ is not small the algorithm produces high resolution images with small approximation error (Figure 2.2). In order to test the performance of our method we test it on different conductivity profiles. We have used iFEM [18] to solve the forward problems.

We also studied the effectiveness of the method on a noisy data set. Figure 2.3 shows the result of the reconstruction when %20 of noise is introduced to the measurement data.

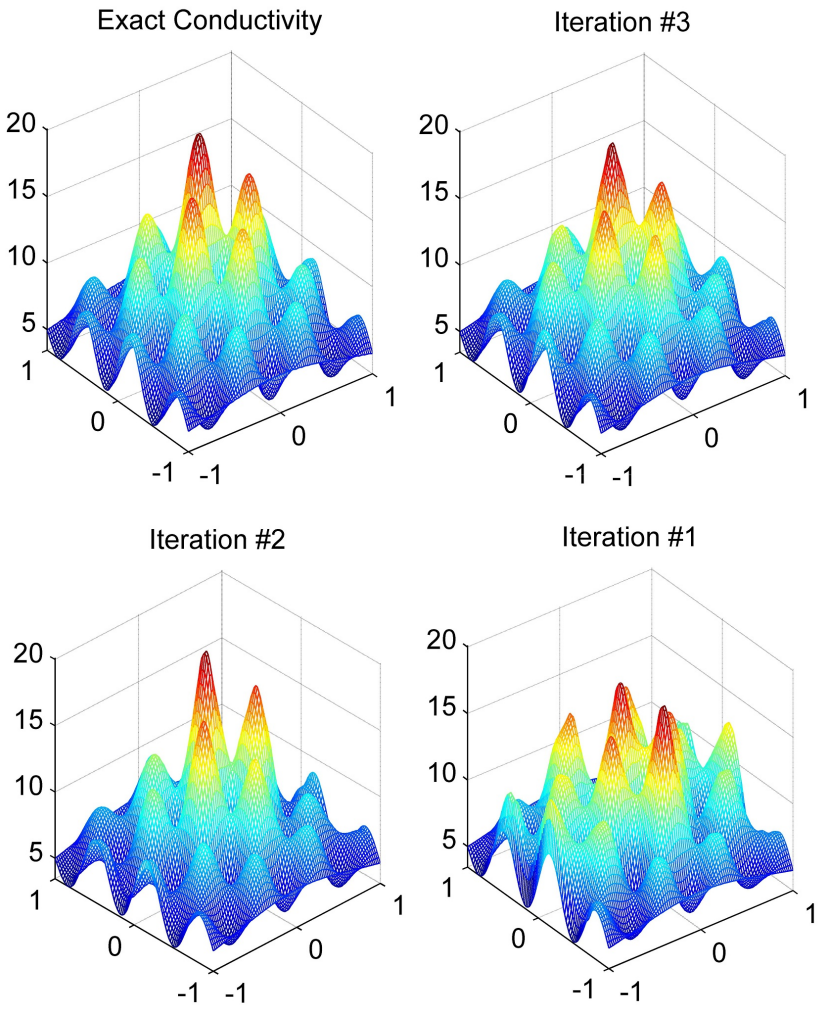

Figure 2.2: Another construction test using a mesh size 64x64. The total L^1 error of the 4^{th} iteration is less than 0.5 which corresponds to 1.5%.

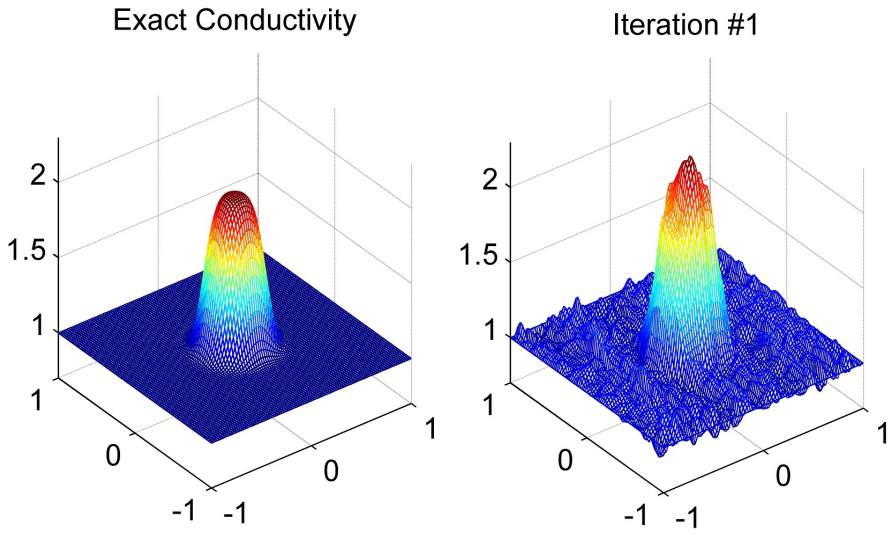

Figure 2.3: The noise level of %20 is introduced to the measurement data.

Chapter 3

GENERAL CASES

3.1 Current Density Imaging in the Anisotropic Case

As noted in the previous chapter the ultrasound waves perturb the conductivity locally and in the isotropic case this is modeled by (2.2). Next, our aim is to give some justification that a similar ultrasound modulation model can also be applied when the conductivity γ is anisotropic, and then to give the mathematical formulation of the problem we are interested in. The main difference with the isotropic case is that our goal is to recover the current density distribution in the object instead of the conductivity.

Let $\Omega \subset \mathbb{R}^n$ be an open, bounded, simply connected domain with smooth boundary which represents a conductive object in the physical setting. Let γ denotes the conductivity tensor which is symmetric and uniformly elliptic, i.e.

$$c|\xi|^2 \leqslant \xi \cdot \gamma\xi \leqslant C|\xi|^2, \qquad \xi \in \mathbb{R}^n,$$

for some constants $0 < c \leqslant C$. The electric potential u solves the anisotropic *conductivity equation*

$$\begin{cases} \sum_{i,j=1}^{n} \frac{\partial}{\partial x_i}\left(\gamma^{i,j}\frac{\partial u}{\partial x_j}\right) = 0 \,\text{in}\, \Omega, \\ u|_{\partial\Omega} = f. \end{cases} \tag{3.1}$$

When we fix a boundary potential on the conductive object we can measure the current response on the boundary. Similar to the isotropic case, the electrical boundary measurements can be represented by the Dirichlet-to-Neumann map which can be defined by

$$\langle \Lambda_\gamma f, g\rangle = \sum_{i,j=1}^{n} \int_\Omega \gamma^{i,j}\frac{\partial u}{\partial x_j}\frac{\partial u_g}{\partial x_i}\mathrm{d}x,$$

where u_g is an extension of g to Ω.

The Drude model ([38]) suggests a motivation to extend the modulation model (2.2) to the anisotropic case. In Drude model the conductivity is given by

$$\gamma = \frac{n_0 e^2}{mg}$$

where n_0 is the number of electrons per unit volume, e is the electron charge, g is the damping constant, and $\frac{1}{m}$ is the inverse of the effective mass tensor. The acoustic waves causes local elastic deformation and assuming this deformation is isotropic, then according to the Drude model, the anisotropy of the effective mass tensor (thus the anisotropy of the conductivity) won't change. The change in the conductivity, thus, can be assumed to be only in the magnitude and proportional to the amplitude of the acoustic signal. More precisely, we assume that the perturbation of the conductivity tensor can be modeled by

$$\gamma_m(x) = (I + mI)\gamma(x) \tag{3.2}$$

where m represents the amplitude of the acoustic signal, and as the physical model suggests we assume it is small and satisfy

$$M^{-1} < 1 + m(x) < M, \quad x \in \Omega.$$

Then the change in the current response of the conductive object to any fixed boundary potential f can be measured on the boundary. This is represented by the map M_f which is defined by

$$M_f(m) := (\Lambda_{\gamma_m} - \Lambda_\gamma)f$$

as in the case of isotropic γ. The inverse problem we are interested in is the following.

Problem 15. *Reconstruction of the current density from the knowledge of M_f for a fixed boundary potential f which is imposed on all or some part of the boundary.*

As noted in the Introduction section the conductivity map has a high contrast and can be very useful for mapping the inhomogeneities. The inhomogeneities of other electrical responses or properties which reflects this high contrast can also be useful especially if its

recovery is more stable and provides an improved resolution. For example Current Density Imaging (CDI) is such technique and can provide a similar internal information about electrical properties of a conductive object. This method is known since [40], [61] where the authors used Magnetic Resonance Imaging (MRI) in order determine the magnetic flux density induced by an applied current. There have been studies on electric conductivity imaging from the internal measurement of current densities [54], [35], [36], [6], [55], [56]. Another reason that we define our problem with the aim to recover the current density is that the recovery of an anisotropic conductivity from one boundary potential is an underdetermined inverse problem. In order to obtain the conductivity itself from M_f one needs more data, i.e. boundary potentials. In [8], [7] the authors study the linearized version of AET in the anisotropic case. Their method requires knowledge of a larger number of internal functionals each of which corresponds to a distinct boundary potential f in our definition above. They gave a local reconstruction method when $\gamma \in C^{1,\alpha}(\bar{\Omega})$ from the power densities of the form $\{\nabla u \cdot \gamma \nabla u : \ u \, \text{is} \, a \, \text{solution to conductivity equation}\}$, and a global reconstruction with assuming existence of admissibility sets that satisfy conditions similar to (2.3).

3.2 A Born-type Approximation

In this section we give an approximation scheme for the problem 15 when the conductivity is close to a constant. Let us denote the current distribution by J so that $(J)_i = \gamma^{i,j} \frac{\partial u}{\partial x_j}$. Testing our measurement operator against a known boundary potential $g \in H^{1/2}(\partial\Omega)$ and an application of divergence theorem yields

$$\begin{aligned} \langle M_f(m), g \rangle &= \sum_{i,j=1}^{n} \int_\Omega \left(\gamma_m^{i,j} \frac{\partial u_m}{\partial x_j} - \gamma^{i,j} \frac{\partial u}{\partial x_j} \right) \frac{\partial u_g}{\partial x_i} \mathrm{d}x \\ &= \int_\Omega m J \cdot \nabla u_g \mathrm{d}x + \sum_{i,j=1}^{n} \int_\Omega \gamma_m^{i,j} \frac{\partial u_d}{\partial x_j} \frac{\partial u_g}{\partial x_i} \mathrm{d}x \end{aligned} \tag{3.3}$$

where $u_d = u_m - u$ is the difference between the modulated and unmodulated potentials, and u_g is an extension of g to Ω.

Note that left hand side is known and we are controlling the modulation m. In addition if we assume that the last term of the above equation is known then the first term on the

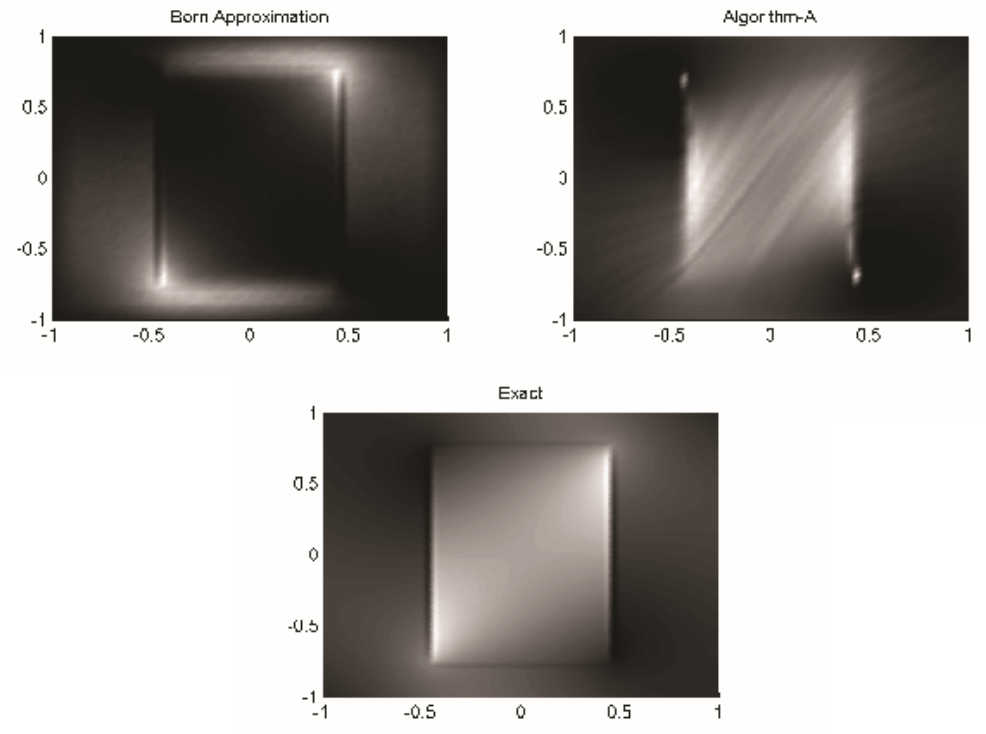

Figure 3.1: Another discontinuous example. The magnitudes of images of approximations J_0, J_0' and exact current distribution J respectively.

right hand side can be used to recover some internal information either by using Fourier transform or by localized ultrasound waves. In particular, when u_g is chosen to be a solution to (3.1) with γ replaced with γ_m then second term on the right hand side of (2.38) vanishes, thus one can recover power densities $J \cdot \nabla u$ by choosing $g = u_m|_{\partial\Omega}$ (see [6] and [7] for a related problem). However in this case the direction information is lost.

Figures 3.3 and 3.4 compares the outputs of two algorithms under different grid sizes. Note that the exact current densities are pictured in the target resolution, that is, an algorithm that recovers the exact current density would give the images shown under the title "Exact". The grid size is not only used for the discretization of the problem but we also use it as acoustic scanning points. The acoustic signals assumed to be focused to the elements. Thus increasing the grid size gives better resolutions however from the practical point of

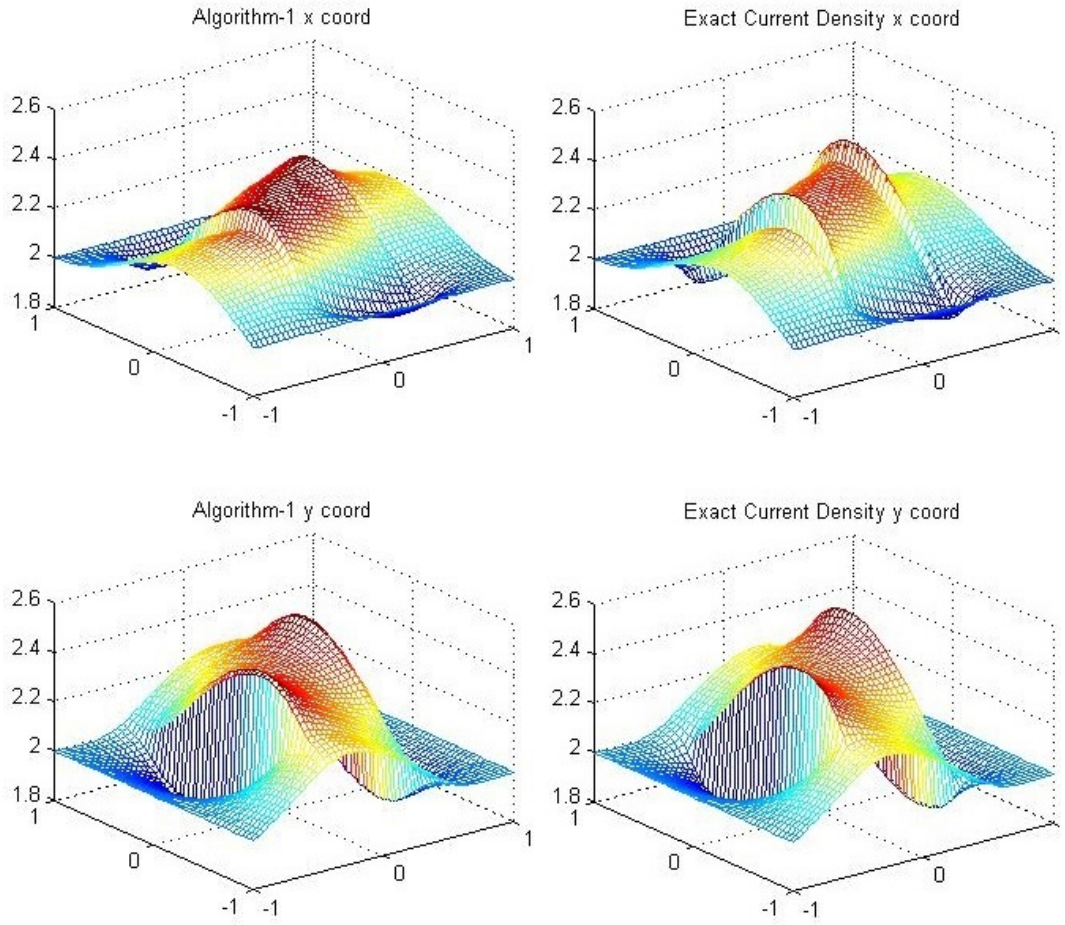

Figure 3.2: x and y coordinates of approximation J_0' and J of the previous example.

view the modulation function is becoming less realistic because of the physical difficulties of focusing ultrasound waves (see Remark below).

Clearly, when γ is a multiple of identity we have

$$\sum_{i,j=1}^{n} \int_{\Omega} \gamma_m^{i,j} \frac{\partial u_d}{\partial x_j} \frac{\partial u_g}{\partial x_i} = \sum_{i,j=1}^{n} \int_{\Omega} m\gamma^{i,j} \frac{\partial u_d}{\partial x_j} \frac{\partial u_g}{\partial x_i} = O(\|m\|_{L^2}^2)$$

if we choose u_g to be the harmonic extension of g. This follows from the fact that $\|u_d\| \leqslant O(\|m\|_{L^2})$. Thus (3.3) becomes

$$\langle M_f(m), g\rangle \;\; = \int_{\Omega} mJ \cdot \nabla u_g \mathrm{d}x + O(\|m\|_{L^2}^2)$$

for any harmonic u_g. Then by a suitable choice of m (one can use focused modulations thus the first term on the right hand side of last equality becomes convolution with approximations of identity, or use oscillatory modulations then apply inverse Fourier transform) it is possible to estimate $J \cdot \nabla u_g$ and thus J since we are free to choose any harmonic function u_g. Then motivated by the Born-approximation, assuming that the "scattering" is not strong thus the harmonic function u_g does not differ substantially from a solution to the conductivity equation, the above scheme can also be used to obtain an approximation to J for anisotropic conductivities close to constant in the sense that

$$\sum_{|\alpha|=1,} \|D^\alpha \gamma^{i,j}\|_{L^2(\Omega)} \leqslant \lambda, \qquad 1 \leqslant i,j \leqslant n \tag{3.4}$$

where α is a multi-index. Moreover let g be the trace of

$$u_g = x_i$$

for some $1 \leqslant i \leqslant n$. We also set $m = m_z$ to be the translations of a smooth mollifier ψ_N, such that

$$m_z(x) = \psi_{j,N}(x - z) \tag{3.5}$$

where

$$\psi_{j,N}(x) = \varepsilon_j N^{-n} \psi(Nx)$$

and $\psi \in C_c^\infty(\mathbb{R}^n)$ is a fixed smooth non-negative function with $\int \psi(x)\mathrm{d}x = 1$ supported in a ball of radius 1. Note that $\int m_z = \varepsilon_j$ and $\|m_z\|_{L^2} = \varepsilon_j \|\psi\|_{L^2}$. Then (3.3) becomes

$$\begin{aligned}
\langle M_f(m), x_i \rangle &= \textstyle\int_\Omega m J_i \mathrm{d}x + \int_\Omega (\gamma_m \nabla u_d)_i \mathrm{d}x \\
&= \textstyle\int_\Omega m J_i \mathrm{d}x - \int_\Omega u_d \nabla \cdot (\gamma_m)_i \mathrm{d}x \\
&= \textstyle\int_\Omega m J_i \mathrm{d}x - \int_\Omega u_d \nabla \cdot \gamma_i \mathrm{d}x - \int_\Omega u_d \nabla \cdot (m\gamma)_i \mathrm{d}x.
\end{aligned}$$

Moreover it is clear that

$$\int_\Omega u_d \nabla \cdot \gamma_i \mathrm{d}x \leqslant C \|m\|_{L^2(\Omega)}$$

and

$$\int_\Omega u_d \nabla \cdot (m\gamma)_i \mathrm{d}x \leqslant C \|m\|^2_{L^2(\Omega)}$$

where C depends on λ. Thus combining these and (3.5) we get

$$|\varepsilon_j^{-1}\psi_{j,N} * J(z) - M_{j,N,z}| \quad \leqslant C\varepsilon_j$$

where

$$M_{j,N,z} = \varepsilon_j^{-1}\langle M_f(m_z), x\rangle$$

when $\operatorname{dist}(x, \partial\Omega) > \frac{1}{N}$ so that $\psi_{j,N}$ is supported in Ω. Note that $M_{j,N,z}$ can be obtained from the measurements. For the sake of brevity, in the above notation the integration (and convolution) of a vector field is carried out for each of the component of the vector field as usual. Then for sufficiently large N $\varepsilon_j^{-1}\psi_{j,N} * J$ gives a reasonable approximation (in L^p, $1 \leqslant p < \infty$) to the unknown vector field J. Thus letting $\varepsilon_j \to 0$ (or in fact $\varepsilon_j < \lambda$ is sufficient) we calculate

$$J_0(z) \quad \approx \ \varepsilon_j^{-1}\langle M_f(m_z), x\rangle \tag{3.6}$$

as an approximation to J, and the error of this approximation is in the order of λ which is defined by (3.4). As noted above, this will be a good approximation when γ is close a homogeneous medium. Similar approximations can be obtained for γ which are close a known isotropic conductivity. In such a case one might replace the harmonic u_g with the CGO solutions of the known conductivity.

Remark. Above, also in the isotropic case, we assumed that the ultrasound waves can be focused to any point in domain Ω. In practice there are difficulties to achieve this, and the resolution of the recovery of the internal data is closely related to the focusing diameter. For example in [3], the recovery of the internal data has accuracy of order $|\omega|^\alpha$ for an $0 \leqslant \alpha < 1/2$ as noted in Proposition 5 above. Using oscillatory waves instead of focuses waves inherit similar type of practical problems.

In [47] authors propose a technique to avoid the use of focused waves through the so called synthetic focusing. The synthetic focusing technique is a step prior to reconstruction of the internal data and it recovers the would be response of the object to the focused modulation from the measurements corresponding to realistic unfocused waves such as spherical waves and plane waves.

For the practical purposes it is also possible to eliminate some of the approximation error of the magnitude $|J_0|$ in (3.6), thus obtaining a slightly better approximation scheme. More precisely, let $\sigma = |J|$ and suppose that $\hat{J} = J/|J|$ is known, then since $\nabla \cdot J = 0$

$$\hat{J} \cdot \nabla\sigma + \nabla \cdot \hat{J}\sigma \quad = \quad 0$$

and σ is known on the boundary of Ω. Thus under suitable conditions (such as the conditions of Lemma 13 F replaced with $\hat{J}$ and γ replaced with σ) one can recover σ. The approximation scheme will contain 2 steps.

i. First approximate to $\widehat{J_0}$ using 3.6,

ii. Recover σ_0 as in the proof of Lemma 13.

Then $J_0' = \sigma\widehat{J_0}$ gives an approximation to the current distribution, and we will refer this approximation scheme as Algorithm A. The recovery of the current distribution works well even when the conductivities are not close to identity as demonstrated in the examples below.

Numerical Examples

In order to study the efficiency of this approach, we have tested both of the methods on different settings in two dimensions. We made our tests using Matlab and iFEM [18] and in most of our examples we use a 64×64 grid and we noted if that is not the case. In the examples domain of interest is a rectangle $[-1, 1] \times [-1, 1]$. Figures 3.6 and 3.7 presents an example with smooth conductivity where we use a fixed boundary potential $f(x, y) = x+y$. See Table 3.1 for the L^1 errors of the both algorithms after we add a noise of 2.5%.

Another example is a conductivity which is continuous in y direction and have jump discontinuities in x direction. We tested with imperfect data and a uniform noise of 10% is introduced to the readings. Born type algorithm fails to recover the current distribution but Algorithm A still gives reasonable results, see Figures 3.1 and 3.2.

		Example 1	Example 2
Algorithm A	:	7.6%	12.8%
Born Approx .	:	8.5%	48.2%
Noise Level		2.5%	10%

Table 3.1: L^1 errors of first two examples.

We also tested a conductivity with constant inclusions. Figure 3.4 and Figure 3.5 shows our example with data without any noise. The L^1 errors of the two algorithms are :

Algorithm A	:	6.8%
Born Approx .	:	7.2%

Although these errors are close to each other, Algorithm A seems to estimate the extreme levels of the current density better, see Figures 3.4 and 3.5.

3.3 Extensions and Notes

3.3.1 Partial data case

Partial data problems are interesting since they are relatively more realistic models compared to full data models. Since hybrid inverse problems usually consist of two steps (recovery of internal data from the boundary measurements and an inverse problem with internal data) partial data might refer to restrictions on boundary measurements and/or internal data. For example, in AET assume that one has access to only a subset Γ of the boundary of the conductive object. Then, electric measurements can be done only on that restricted part of the boundary. The uniqueness given by Proposition 10 in the isotropic case provides some understanding for this kind of partial measurements. Another type of partial data problem occurs when the ultrasound scanning is restricted to some sub-domain of Ω. We now give a non-uniqueness for anisotropic case for this type of partial data problem.

It is clear that in general the uniqueness of the anisotropic problem depends on the boundary potential f. For example a constant boundary potential f will make $M_f(m)$ vanish for every possible m. In the isotropic case we know that such examples (more precisely, the ones which doesn't satisfy the conditions of Proposition 10) are the only exceptions to uniqueness, but in the anisotropic case we don't know if a similar result holds. However the partial data problem inherit the non-uniqueness from the Calderón problem. Based on the transformation optics, in [33], it is shown that that there are distinct conductivities whose Dirichlet-to-Neumann maps coincide. Since then transformation optics has been a popular research topic and, based on it, there has been many research on the theory and applications of invisibility and cloaking [32], [27], [28], [29], [49], [52], [51], [44], [59] (see [30] and its references for an extensive list).

Let $\psi : \bar{\Omega} \to \bar{\Omega}$ be a C^∞ diffeomorphism with $\psi|_{\partial\Omega} = I$, where I denotes the identity map. Then, given an anisotropic conductivity map γ on Ω, define a new conductivity map $\tilde{\gamma}$ by the push-forward of γ in ψ, that is

$$\tilde{\gamma} = \psi_*\gamma = \left(\frac{(D\psi)^T \circ \gamma \circ (D\psi)}{|\det D\psi|} \right) \circ \psi^{-1}. \tag{3.7}$$

It is known that

$$\Lambda_\gamma = \Lambda_{\tilde{\gamma}},$$

thus there is an infinite set of conductivities such that the Dirichlet-to-Neumann maps coincide. This well known fact also gives a non-uniqueness for the anisotropic AET problem with partial data. Suppose an open sub-domain $\omega \subset \Omega$ is not reachable by the ultrasound scanning. Thus all the experiments mentioned in the definition of the problem can be done on $\Omega \backslash \bar{\omega}$ and one can ask to recover the current distribution from the knowledge of

$$M_f(m), \quad \operatorname{supp} m \subset \Omega \backslash \bar{\omega}.$$

Let us fix a C^∞ diffeomorphism $\psi : \bar{\Omega} \to \bar{\Omega}$ such that $\psi|_{\bar{\Omega}\backslash\omega} = I$ and $\psi|_{\partial\Omega} = I$. Then we claim that the modulated conductivities $\gamma_m(x) = (1 + m(x))\gamma(x)$ and $\tilde{\gamma}_m(x) = (1 + m(x))\tilde{\gamma}(x)$ have same Dirichlet-to-Neumann map. This immediately follows from the fact

that $\tilde{\gamma}$, defined by the push-forward (3.7), has the same Dirichlet-to-Neumann map as γ, which implies

$$\begin{aligned}
\tilde{\gamma}_m &= (1+m(x))\tilde{\gamma}(x) \\
&= (1+m(x))\left(\frac{(D\psi)^T \circ \gamma \circ (D\psi)}{|\det D\psi|}\right) \circ \psi^{-1}(x) \\
&= \left(\frac{(D\psi)^T \circ (1+m(x))\gamma \circ (D\psi)}{|\det D\psi|}\right) \circ \psi^{-1}(x) \\
&= \psi_* \gamma_m
\end{aligned}$$

since $(1+m(x))$ is scalar and supported in $\Omega\backslash\bar{\omega}$, and ψ is identity on its support. Thus

$$\Lambda_{\gamma_m} = \Lambda_{\tilde{\gamma}_m},$$

which in turn implies

$$M_f(m) = \tilde{M}_f(m),$$

therefore we don't have a uniqueness for AET problem with partial data.

3.3.2 Electromagnetic case

In this section we give an inverse problem motivated by the AET and give an approximation to an internal data. For the Maxwell's equations we denote the conductivity by $\sigma(x)$, the electric permittivity by $\varepsilon(x)$ and the magnetic permeability by $\mu(x)$. We assume all are isotropic bounded functions in Ω, and Ω is an open bounded domain in $\mathbb{R}^3$ with smooth boundary. We consider the electromagnetic fields (E, H) which satisfy the time independent Maxwell's equations

$$\begin{aligned}
\Lambda \times E &= i\omega\mu H, \\
\Lambda \times H &= -i\omega\varepsilon E + \sigma E,
\end{aligned} \tag{3.8}$$

in Ω, where $\omega > 0$ is the time-harmonic frequency of the fields. We also assume σ, ε and μ are $C^2(\bar{\Omega})$ functions. The inverse conductivity problem can be generalized to the time-harmonic Maxwell's equations, and in this case the goal is to recover the electromagnetic

parameters σ, ε, μ from the knowledge of boundary mapping Λ which is defined by

$$\Lambda : \nu \times E|_{\partial\Omega} \mapsto \nu \times H|_{\partial\Omega}$$

where ν is the outward unit normal vector to $\partial\Omega$. See [62], [57], [58] for the properties of the problem, and [70] for a review of inverse boundary problems for electromagnetic waves. The above problem is first defined in [62] where they gave an approximate constructive recovery procedure for the linearized problem. $TH^s(\partial\Omega)$ denotes the space of tangential vector fields on $\partial\Omega$ with components in the Sobolev space $H^s(\partial\Omega)$. It is well known that except for a discrete set of resonant frequencies (in the non dissipative case $\sigma = 0$), the forward problem admits a unique solution, and

$$\Lambda : TH^{1/2}(\partial\Omega) \to TH^{-1/2}(\partial\Omega)$$

is a well defined map. In this section we assume that ω is not a resonant frequency. Let us assume that, motivated by the electro-acoustic effect, it is possible to make local elastic deformations which creates a change in the electromagnetic parameters, that is, we assume that these deformations change the conductivity as in the steady current case. The modulated conductivity is given by

$$\sigma_m(x) = (1 + m(x))\sigma(x).$$

Once again we set $M_f(m) := \Lambda_m f - \Lambda f$ for some fixed $f \in TH^{1/2}(\partial\Omega)$, and then our inverse problem is :

Problem 16. *Reconstruction of the electromagnetic properties σ, ε and μ from the knowledge of M_f.*

We consider the problem in a slightly different framework. Suppose that all three electromagnetic coefficients can be locally perturbed, and let $\tilde{\sigma}, \tilde{\varepsilon}$ and $\tilde{\mu}$ denotes the conductivity, permittivity and permeability after the deformation. For the sake of brevity in the below calculations we use $d = -\varepsilon + \sigma/i\omega$ and $\tilde{d} = -\tilde{\varepsilon} + \tilde{\sigma}/i\omega$. Suppose that (E, H)

is the solution to (3.8) with $f = \nu \times E|_{\partial\Omega}$ for some fixed $f \in TH^{1/2}(\partial\Omega)$. Similarly the electromagnetic fields $(\tilde{E}, \tilde{H})$ denote the solution to (3.8) with $\nu \times \tilde{E}|_{\partial\Omega} = f$ where σ, ε,μ are replaced with $\tilde{\sigma}, \tilde{\varepsilon}$ and $\tilde{\mu}$, respectively. We use the subscript d notation for the differences between the perturbed and the initial fields,

$$E_d := \tilde{E} - E, \qquad H_d := \tilde{H} - H,$$

and similarly for the coefficients

$$\mu_d = \tilde{\mu} - \mu, \qquad d_d = \tilde{d} - d.$$

Then a straightforward calculation shows

$$\begin{aligned} \Lambda \times E_d &= i\omega\mu H_d + i\omega\mu_d \tilde{H}, \\ \Lambda \times H_d &= i\omega d E_d + i\omega d_d \tilde{E}. \end{aligned}$$

Since we have access to $\nu \times E_d|_{\partial\Omega} \mapsto \nu \times H_d|_{\partial\Omega}$ on the boundary, we can measure

$$\begin{aligned} \int_{\partial\Omega} \nu \cdot (E_d \times A) &= \int_\Omega \nabla \cdot (E_d \times A), \\ &= \int_\Omega \nabla \times E_d \cdot A - E_d \cdot \nabla \times A, \\ &= \int_\Omega i\omega(\mu H_d + \mu_d \tilde{H}) \cdot A - E_d \cdot \nabla \times A. \end{aligned}$$

Similarly

$$\begin{aligned} \textstyle\int_{\partial\Omega} \nu \cdot (H_d \times B) &= \textstyle\int_\Omega \nabla \times H_d \cdot B - H_d \cdot \nabla \times B, \\ &= \textstyle\int_\Omega i\omega(d E_d + d_d \tilde{E}) \cdot B - H_d \cdot \nabla \times B, \end{aligned}$$

Then

$$\begin{aligned} \textstyle\int_{\partial\Omega} \nu \cdot (E_d \times A + H_d \times B) &= \textstyle\int_\Omega \nabla \times H_d \cdot B - H_d \cdot \nabla \times B, \\ &= \textstyle\int_\Omega i\omega d_d \tilde{E} \cdot B + i\omega\mu_d \tilde{H} \cdot A \\ &\quad + \textstyle\int_\Omega E_d \cdot (i\omega d B - \nabla \times A) + H_d \cdot (i\omega\mu A - \nabla \times B). \end{aligned}$$

As motivated by AET, where we had control over the perturbation, if we assume (B, A) is another solution to our system, that is

$$\begin{aligned} \Lambda \times B &= i\omega\mu A, \\ \Lambda \times A &= i\omega dB, \end{aligned}$$

then the last integral above vanishes, and we can conclude that from the measurements one can obtain the functionals of the form

$$\int_\Omega i\omega d_d \tilde{E} \cdot B + i\omega\mu_d \tilde{H} \cdot A.$$

In particular if we assume $(B, A) = (E, H)$ and also assume the knowledge of measurements for more than one non resonant frequencies, then one can approximate to internal data $\sigma E \cdot E$ and $\mu H \cdot H - \varepsilon E \cdot E$. In a more restricted case if we assume we can only perturb the conductivity (as in the case of AET) then internal data $\sigma E \cdot E$ can be approximated from the boundary measurements.

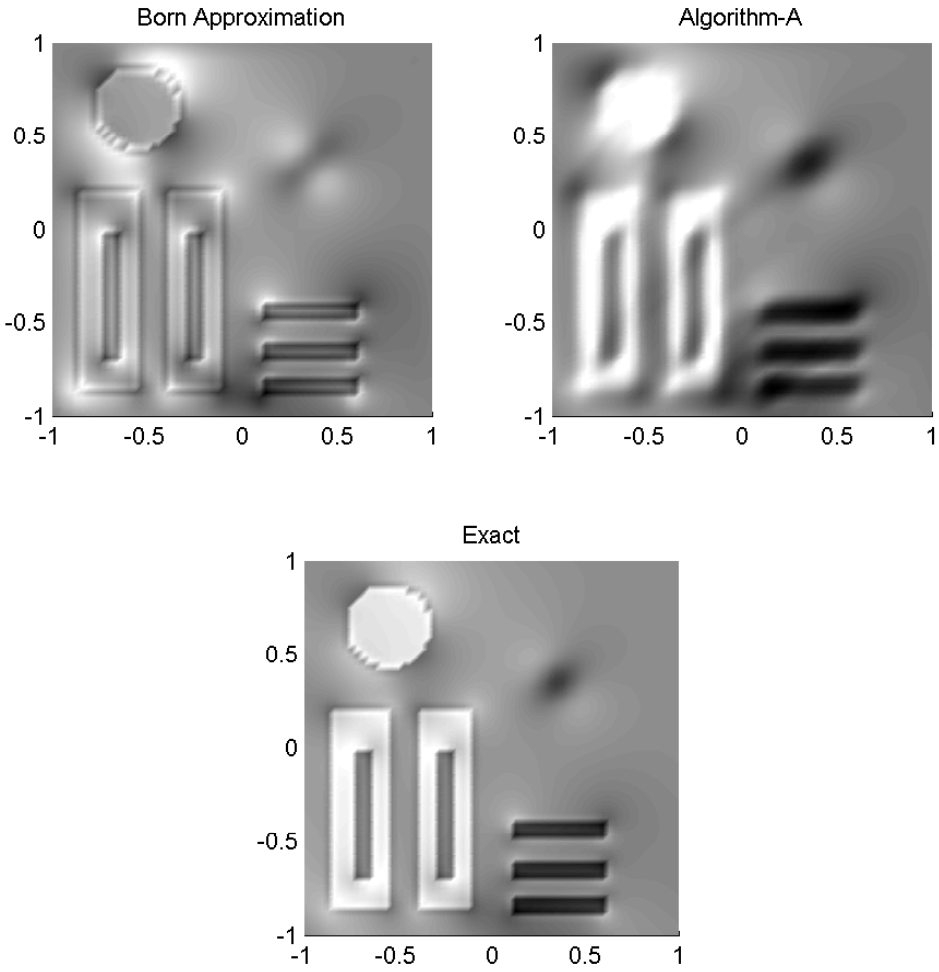

Figure 3.3: The images of the magnitude of the approximations $|J_0|, |J_0'|$ and exact current distribution $|J|$, respectively. The grid size 64×64.

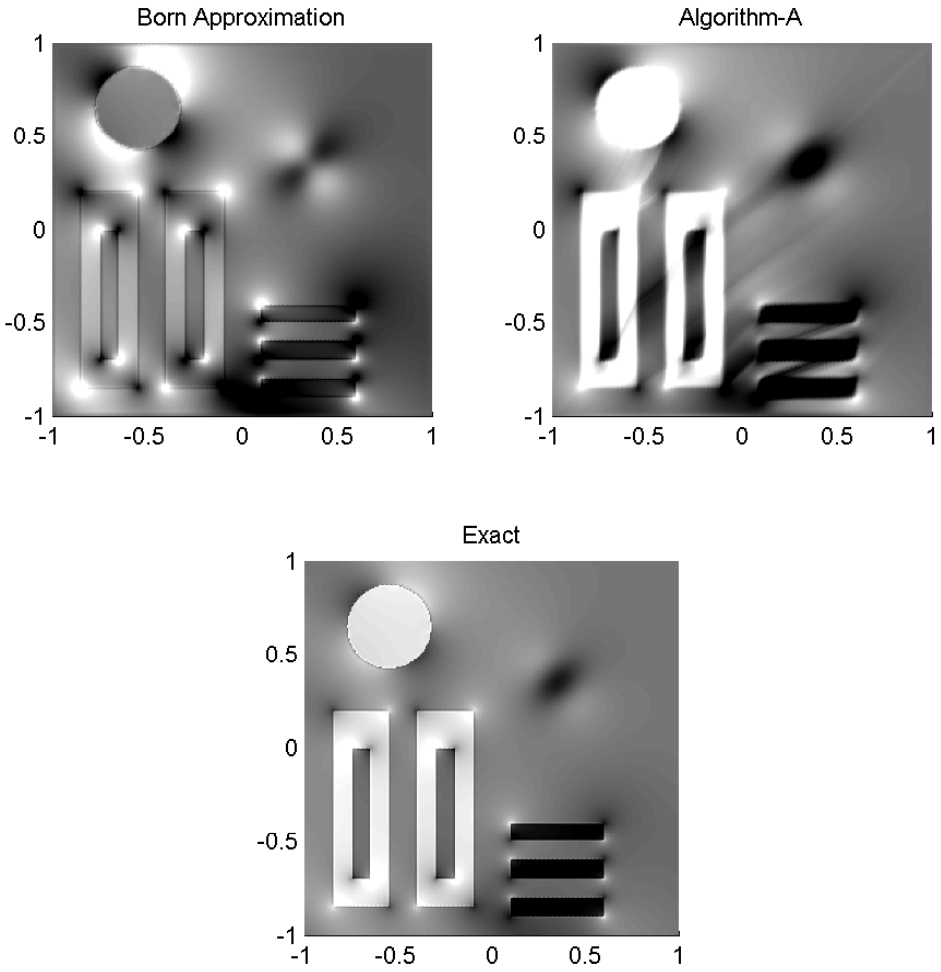

Figure 3.4: The images of the magnitude of the approximations $|J_0|, |J_0'|$ and exact current distribution $|J|$, respectively. The grid size is 256×256.

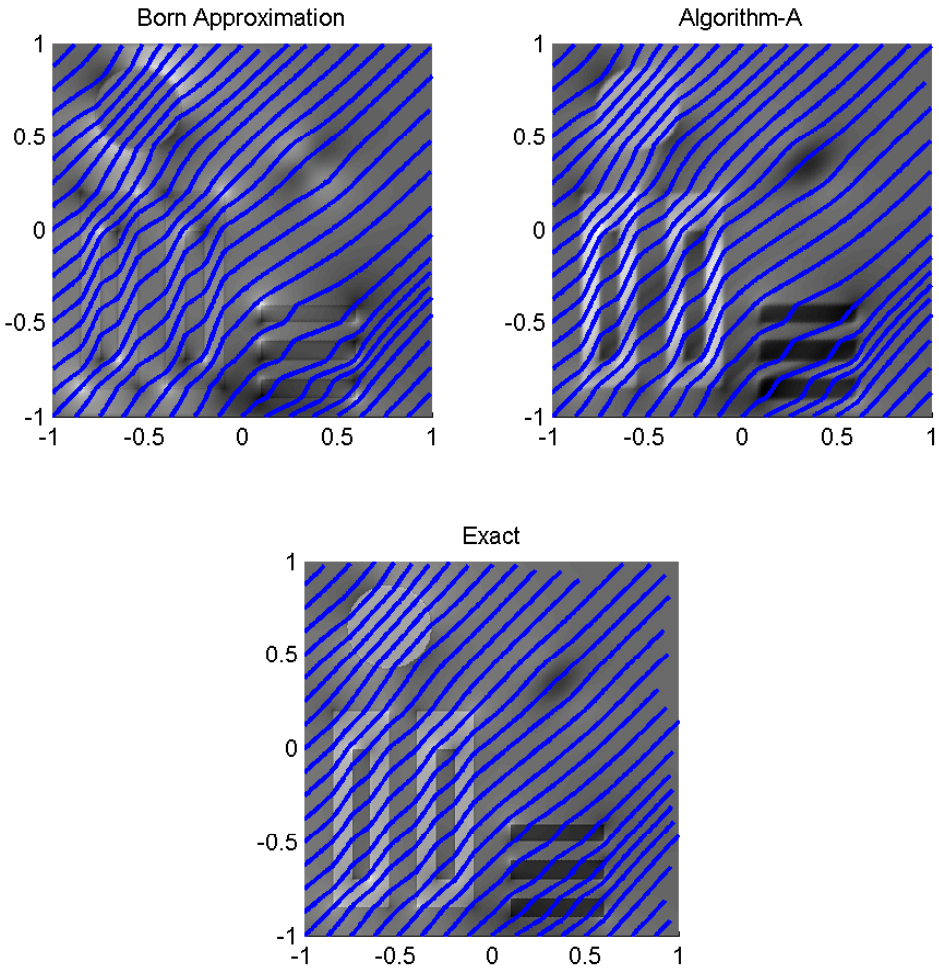

Figure 3.5: The magnitudes and integral curves of images of approximations J_0, J_0' and exact current distribution J respectively.

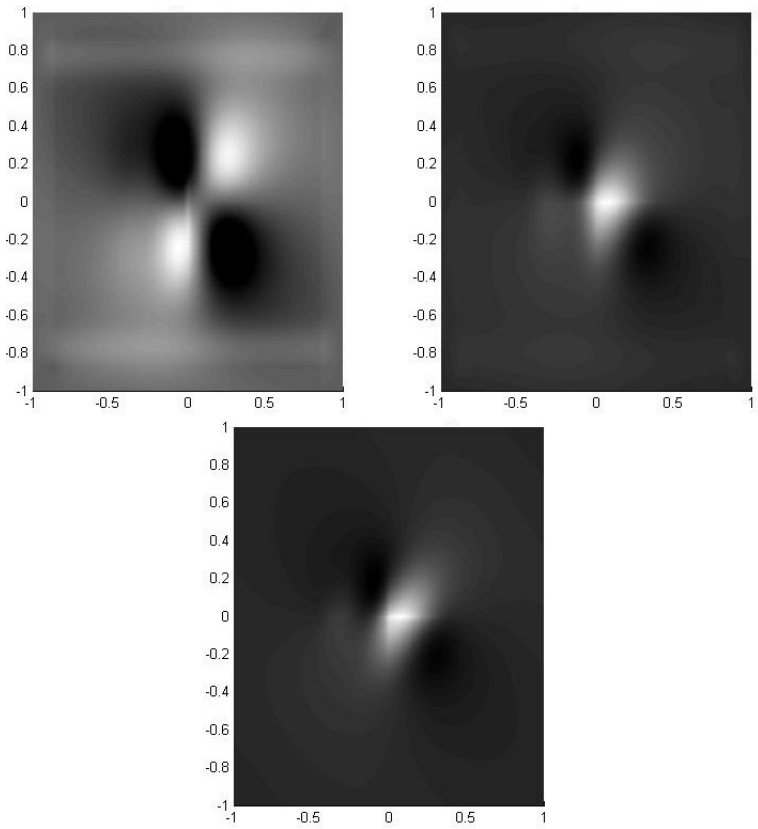

Figure 3.6: A smooth conductivity example. The magnitudes of images of approximations J_0, J_0' and exact current distribution J respectively.

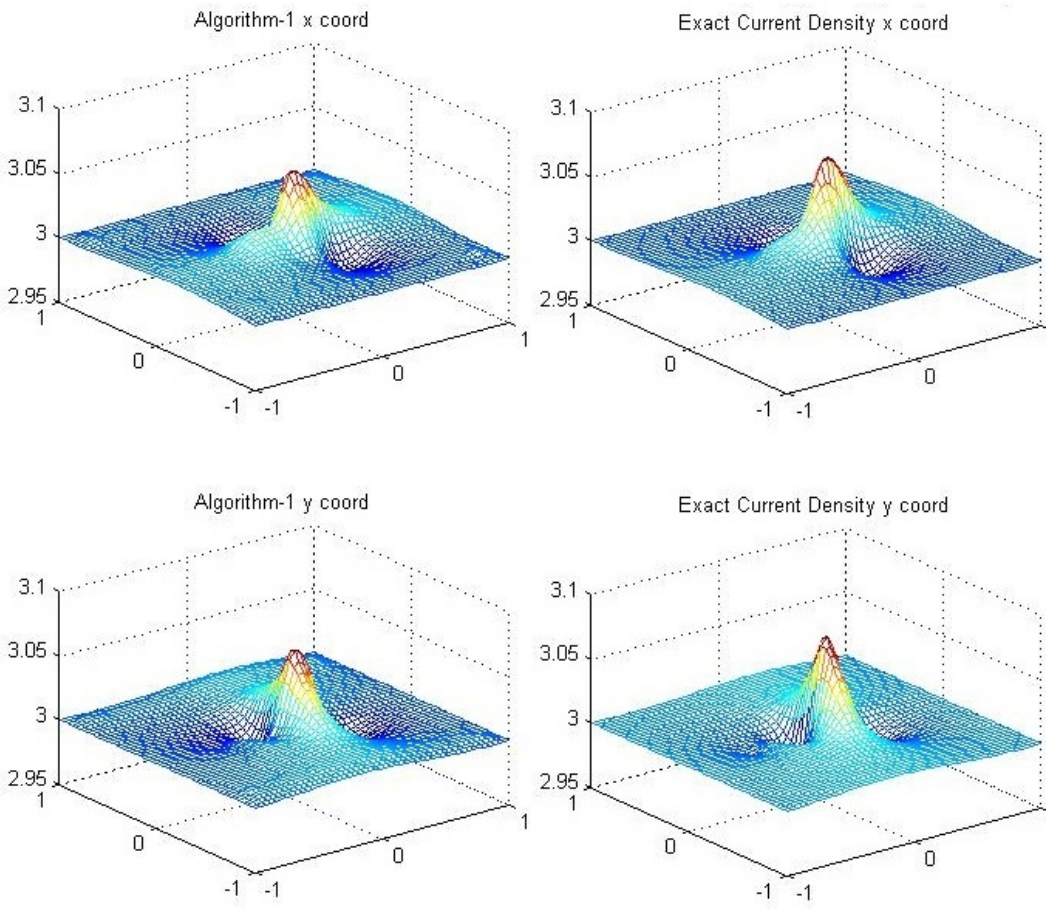

Figure 3.7: x and y coordinates of approximation J_0' and J of the previous example.

BIBLIOGRAPHY

[1] Giovanni Alessandrini. Stable determination of conductivity by boundary measurements. *Applicable Analysis*, 27:153–172, 1988.

[2] Giovanni Alessandrini and Vincenzo Nesi. Univalent -harmonic mappings. *Archive for Rational Mechanics and Analysis*, 158(2):155–171, 2001.

[3] Habib Ammari, Eric Bonnetier, Yves Capdeboscq, Mickal Tanter, and Mathias Fink. Electrical impedance tomography by elastic deformation. *Siam Journal on Applied Mathematics*, 68:1557–1573, 2008.

[4] Guillaume Bal. Cauchy problem and ultrasound modulated EIT. To appear in Analysis & PDE, 2012.

[5] Guillaume Bal, Eric Bonnetier, Francois Monard, and Faouzi Triki. Inverse diffusion from knowledge of power densities. Preprint, 2011.

[6] Guillaume Bal, Chenxi Guo, and Francois Monard. Inverse anisotropic conductivity from internal current densities. 2013.

[7] Guillaume Bal and Francois Monard. Inverse anisotropic conductivity from power densities in dimension $n \geq 3$. 2012.

[8] Guillaume Bal and Francois Monard. Inverse anisotropic diffusion from power density measurements in two dimensions. *Inverse Problems*, 28(8):084001, 2012.

[9] Guillaume Bal and Francois Monard. Inverse diffusion problems with redundant internal information. *Inverse Problems and Imaging*, 6(2):289–313, 2012.

[10] Guillaume Bal, Kui Ren, Gunther Uhlmann, and Ting Zhou. Quantitative thermoacoustics and related problems. *Inverse Problems*, 27(5):055007, 2011.

[11] Guillaume Bal and Gunther Uhlmann. Inverse diffusion theory of photoacoustics. *Inverse Problems*, 26(8):085010, 2010.

[12] Gang Bao and Hongyu Liu. Nearly cloaking the full maxwell equations. preprint.

[13] A. G. Bell. On the Production and Reproduction of Sound by Light. *American Journal of Sciences*, XX(118):305–324, October 1880.

[14] Liliana Borcea. Electrical impedance tomography. *Inverse Problems*, 18(6):R99, 2002.

[15] Alexander Bukhgeim and Gunther Uhlmann. Recovering a potential from partial cauchy data. *Communications in Partial Differential Equations*, 27(3-4):653–668, -4/2002.

[16] Alberto P. Calderón. On an inverse boundary value problem. *Seminar on Numerical Analysis and its Applications to Continuum Physics*, pages 65–73, 1980.

[17] Y. Capdeboscq, J. Fehrenbach, F. de Gournay, and O. Kavian. Imaging by modification: Numerical reconstruction of local conductivities from corresponding power density measurements. *SIAM J. Imaging Sci.*, 2(4):1003–1030, 2009.

[18] Long Chen. iFEM: an innovative finite element methods package in MATLAB. *In Preparation*, 2008.

[19] Margaret Cheney, David Isaacson, and Jonathan C. Newell. Electrical impedance tomography. *SIAM Review*, 41:85–101, 1999.

[20] Earl A. Coddington and Norman Levinson. *Theory of ordinary differential equations*. McGraw-Hill, New York, 1972.

[21] Committee on the Mathematics and Physics of Emerging Dynamic Biomedical Imaging, National Research Council. *Mathematics and Physics of Emerging Biomedical Imaging*. The National Academies Press, 1996.

[22] L.C. Evans. *Partial Differential Equations*. Graduate Studies in Mathematics. American Mathematical Society, 2010.

[23] Joel Feldman and Gunther Uhlmann. Inverse problems. *Book Draft*.

[24] C Gabriel, S Gabriel, and E Corthout. The dielectric properties of biological tissues: I. literature survey. *Physics in Medicine and Biology*, 41(11):2231, 1996.

[25] Bastian Gebauer and Otmar Scherzer. Impedance-acoustic tomography. *SIAM Journal of Applied Mathematics*, 69(2):565–576, 2008.

[26] David Gilbarg and Neil S. Trudinger. *Elliptic partial differential equations of second order*. Classics in mathematics. Springer, 2001.

[27] Allan Greenleaf, Yaroslav Kurylev, Matti Lassas, and Gunther Uhlmann. Improvement of cylindrical cloaking with the shs lining. *Opt. Express*, 15(20):12717–12734, Oct 2007.

[28] Allan Greenleaf, Yaroslav Kurylev, Matti Lassas, and Gunther Uhlmann. Mathematics of invisibility. *Journes quations aux drives partielles*, pages 1–11, 6 2007.

[29] Allan Greenleaf, Yaroslav Kurylev, Matti Lassas, and Gunther Uhlmann. Cloaking devices, electromagnetic wormholes, and transformation optics. *SIAM Review*, 51(1):3–33, 2009.

[30] Allan Greenleaf, Yaroslav Kurylev, Matti Lassas, and Gunther Uhlmann. Invisibility and Inverse Problems. *Bull. Amer. Math. Soc.*, 46:55–97, 2009.

[31] Allan Greenleaf, Yaroslav Kurylev, Matti Lassas, and Gunther Uhlmann. Invisibility and inverse problems. *Bull. Am. Math. Soc., New Ser.*, 46(1):55–97, 2009.

[32] Allan Greenleaf, Matti Lassas, and Gunther Uhlmann. Anisotropic conductivities that cannot be detected by EIT. *Physiological Measurement*, 24(2):413, 2003.

[33] Allan Greenleaf, Matti Lassas, and Gunther Uhlmann. On nonuniqueness for Calderón's inverse problem. *Math. Res. Lett.*, 10:685–693, July 2003.

[34] R. Hardt, M. Hoffmann, T. Hoffmann, and N. Nadirashvili. Critical sets of solutions to elliptic equations. *J. Differential Geom.*, 51:pp. 359–373, 1999.

[35] Karshi F Hasanov, Angela W. Ma, Adrian I. Nachman, and Michael L.G. Joy. Current density impedance imaging. *IEEE Trans Med Imaging*, 27(9):1301–1309, 2008.

[36] Nicholas Hoell, Amir Moradifam, and Adrian I. Nachman. Current density impedance imaging of an anisotropic conductivity in a known conformal class. 2013.

[37] Victor Isakov. *Inverse problems for partial differential equations*. Applied mathematical sciences. Springer, 1998.

[38] John D. Jackson. *Classical Electrodynamics Third Edition*. Wiley, third edition, August 1998.

[39] Jacques Jossinet. The impedivity of freshly excised human breast tissue. *Physiological Measurement*, 19(1):61, 1998.

[40] M. Joy, G. Scott, and M. Henkelman. In vivo detection of applied electric currents by magnetic resonance imaging. *Magnetic Resonance Imaging*, 7(1):89 – 94, 1989.

[41] Carlos E. Kenig, Johannes Sjoestrand, and Gunther Uhlmann. The Calderón problem with partial data. *The Annals of Mathematics*, 165:567–591, 2004.

[42] Kim Knudsen, Matti Lassas, Jennifer L. Mueller, and Samuli Siltanen. Regularized d-bar method for the inverse conductivity problem. *Inverse Problems and Imaging*, 3(4):599–624, 2009.

[43] Ilker Kocyigit. Acousto-electric tomography and CGO solutions with internal data. *Inverse Problems*, 28(12):125004, 2012.

[44] Ilker Kocyigit, Hongyu Liu, and Hongpeng Sun. Regular scattering patterns from near-cloaking devices and their implications for invisibility cloaking. *Inverse Problems*, 29(4):045005, 2013.

[45] Robert Kohn and Michael Vogelius. Determining conductivity by boundary measurements. *Communications on Pure and Applied Mathematics*, 37(3):289–298, 1984.

[46] Peter Kuchment and Leonid Kunyansky. Mathematics of photoacoustic and thermoacoustic tomography. *Springer Handbook of Mathematical Methods in Imaging*, (520):819–865, 2009.

[47] Peter Kuchment and Leonid Kunyansky. Synthetic focusing in ultrasound modulated tomography. *Inverse Problems and Imaging*, 4(4):665–673, 2010.

[48] Peter Kuchment and Leonid Kunyansky. 2D and 3D reconstructions in acousto-electric tomography. *Inverse Problems*, 27(5):055013, 2011.

[49] Ulf Leonhardt. Optical conformal mapping. *Science*, 312(5781):1777–1780, 2006.

[50] Niculae Mandache. Exponential instability in an inverse problem for the schrdinger equation. *Inverse Problems*, 17(5):1435, 2001.

[51] Graeme W Milton, Marc Briane, and John R Willis. On cloaking for elasticity and physical equations with a transformation invariant form. *New Journal of Physics*, 8(10):248, 2006.

[52] Graeme W Milton and Nicolae-Alexandru P Nicorovici. On the cloaking effects associated with anomalous localized resonance. *Proceedings of the Royal Society A: Mathematical, Physical and Engineering Science*, 462(2074):3027–3059, 2006.

[53] Adrian I. Nachman. Reconstructions from boundary measurements. *The Annals of Mathematics*, 128(3):pp. 531–576, 1988.

[54] Adrian I. Nachman, Alexandru Tamasan, and Timonov Alexandar. Current density impedance imaging. *Contemporary Mathematics of the American Mathematical Society*, 559:135–150, 2011.

[55] Adrian I. Nachman, Alexandru Tamasan, and Alexandre Timonov. Conductivity imaging with a single measurement of boundary and interior data. *Inverse Problems*, 23(6):2551, 2007.

[56] Adrian I. Nachman, Alexandru Tamasan, and Alexandre Timonov. Recovering the conductivity from a single measurement of interior data. *Inverse Problems*, 25(3):035014, 2009.

[57] Petri Ola, Lassi Päivärinta, and Erkki Somersalo. An inverse boundary value problem in electrodynamics. *Duke Math. J.*, 70(3):617–653, 1993.

[58] Petri Ola and Erkki Somersalo. Electromagnetic inverse problems and generalized sommerfeld potential. *SIAM J. Appl. Math.*, 56:1129–1145, 1996.

[59] J. B. Pendry, D. Schurig, and D. R. Smith. Controlling electromagnetic fields. *Science*, 312(5781):1780–1782, 2006.

[60] O. Scherzer. *Handbook of Mathematical Methods in Imaging: Vol. 1*. Springer Reference. Springer, 2011.

[61] G.C. Scott, M. L G Joy, R.L. Armstrong, and R. M. Henkelman. Measurement of nonuniform current density by magnetic resonance. *Medical Imaging, IEEE Transactions on*, 10(3):362–374, 1991.

[62] Erkki Somersalo, David Isaacson, and Margaret Cheney. A linearized inverse boundary value problem for maxwell's equations. *Journal of Computational and Applied Mathematics*, 42(1):123 – 136, 1992.

[63] Plamen Stefanov and Gunther Uhlmann. Thermoacoustic tomography with variable sound speed. *Inverse Problems*, 25(7):075011, 2009.

[64] Plamen Stefanov and Gunther Uhlmann. Thermoacoustic tomography arising in brain imaging. *Inverse Problems*, 27(4):045004, 2011.

[65] John Sylvester and Gunther Uhlmann. A uniqueness theorem for an inverse boundary value problem in electrical prospection. *Communications on Pure and Applied Mathematics*, 39(1):91–112, 1986.

[66] John Sylvester and Gunther Uhlmann. A global uniqueness theorem for an inverse boundary value problem. *The Annals of Mathematics*, 125(1):pp. 153–169, 1987.

[67] Michael E. Taylor. *Partial Differential Equations: Basic Theory*. Springer, New York, 1996.

[68] Gunther Uhlmann. Electrical impedance tomography and Calderón's problem. *Inverse Problems*, 25(12):123011, 2009.

[69] Gunther Uhlmann. Visibility and invisibility. *ICIAM 07-6th International Congress on Industrial and Applied Mathematics*, 18(4):381–408, 2009.

[70] Gunther Uhlmann and Ting Zhou. Inverse electromagnetic problems. to appear in the Encyclopedia of Applied and Computational Mathematics.

[71] Lihong V. Wang and Hsin i Wu. *Biomedical Optics: Principles and Imaging*. Wiley, 2007.

[72] Hao Zhang and Lihong V. Wang. Acousto-electric tomography. volume 5320, pages 145–149. SPIE, 2004.

[73] Y Zou and Z Guo. A review of electrical impedance techniques for breast cancer detection. *Medical Engineering and Physics*, 25(2):79–90, 2003.